

PEPTIDE-INDUCED AMYLOIDOSIS OF RECOMBINANT HUMAN  
PRION PROTEIN

THESIS

Presented to the Graduate Council of  
Texas State University-San Marcos  
in Partial Fulfillment  
of the Requirements

for the Degree

Master of SCIENCE

by

Melody Christine Adam, B.S.

San Marcos, Texas  
May 2012

PEPTIDE-INDUCED AMYLOIDOSIS OF RECOMBINANT HUMAN  
PRION PROTEIN

Committee Members Approved:

---

Steven Whitten, Chair

---

Rachell Booth

---

Wendi David

Approved:

---

J. Michael Willoughby  
Dean of the Graduate College

**COPYRIGHT**

by

Melody Christine Adam

2012

## **FAIR USE AND AUTHOR'S PERMISSION STATEMENT**

### **Fair Use**

This work is protected by the Copyright Laws of the United States (Public Law 94-553, section 107). Consistent with fair use as defined in the Copyright Laws, brief quotations from this material are allowed with proper acknowledgement. Use of this material for financial gain without the author's express written permission is not allowed.

### **Duplication Permission**

As the copyright holder of this work I, Melody Christine Adam, authorize duplication of this work, in whole or in part, for educational or scholarly purposes only.

**TO MY FATHER**

## **ACKNOWLEDGEMENTS**

First and foremost, I would like to thank my advisor, Dr. Steven Whitten, for all of his support and guidance. I would not have been able to complete this without his insightful ideas or words of encouragement. It was a pleasure working for such an extremely intelligent individual. I would also like to acknowledge my committee members, which include Dr. Rachell Booth and Dr. Wendi David, for their critical review of my research project. Finally, special thanks to my student colleague, James Campbell, who helped me in many ways.

This manuscript was submitted on January 3, 2012.

## TABLE OF CONTENTS

	<b>Page</b>
ACKNOWLEDGEMENTS .....	vi
LIST OF TABLES .....	x
LIST OF FIGURES .....	xi
ABSTRACT .....	xiii
CHAPTER	
I. INTRODUCTION .....	1
1.1 Amyloidosis Disorders .....	2
1.2 Structural Models of Amyloid .....	2
1.3 Amyloidosis Induced by Peptide Binding .....	6
1.4 Research Goals .....	10
II. MATERIALS AND METHODS .....	13
2.1 Materials .....	13
2.2 Cloning, Over-Expression, and Purification of Recombinant Human Prion Protein .....	13
2.2.1 Cloning and transformation of bacterial cell cultures .....	13
2.2.2 Glycerol stocks of transformed E. coli cells for long term storage at -80°C .....	15

2.2.3	Bacterial over-expression of recombinant hPrP .....	16
2.2.4	Purification of recombinant hPrP from E. coli cells .....	17
2.3	Protein Detection Methods .....	20
2.3.1	Sodium dodecyl sulfate polyacrylamide gel electrophoresis (SDS-PAGE).....	20
2.3.2	Silver nitrate staining of polyacrylamide electrophoresis gels .....	22
2.3.3	Western Blot detection of hPrP.....	25
2.3.4	Estimating hPrP concentration by absorbance spectroscopy at 280 nm.....	25
2.4	Amyloid Detection Methods.....	27
2.4.1	Detecting amyloid by resistance to Proteinase K digestion.	27
2.4.2	Detecting amyloid by Thioflavin T fluorescence .....	29
2.4.3	Detecting amyloid by light scattering at 400 nm .....	29
2.4.4	Detecting amyloid by circular dichroism spectropolarimetry .....	32
2.4.5	Estimating the amount of hPrP amyloid in a sample by the Bradford Assay .....	35
2.5	Methods to Promote the Structural Conversion of Natively-Folded Recombinant hPrP to Amyloid Oligomers .....	36
2.5.1	De novo amyloidosis induced by peptide:hPrP binding interactions.....	36
2.5.2	Amyloidosis induced by providing amyloid particles as nucleating seeds .....	37
III.	AMYLOID MISFOLDING OF NATIVE RECOMBINANT HUMANPRION PROTEIN INDUCED BY PEPTIDE INTERACTIONS .....	39
3.1	Introduction .....	39
3.2	Results and Discussion .....	40
3.2.1	Purification and native folding of recombinant hPrP .....	40

3.2.2 Peptide-induced amyloidosis of recombinant hPrP .....	41
3.2.3 Non-amyloid aggregation of recombinant hPrP .....	52
3.2.4 hPrP amyloidosis through amyloid seeding.....	52
3.3 Conclusions.....	57
IV. PEPTIDE HOMOLOGS TO THE RF-AMIDE CLASS OF NEURO- PEPTIDES INDUCE AMYLOID MISFOLDING OF RECOMBINANT HUMAN PRION PROTEIN .....	60
4.1 Introduction.....	60
4.2 Results and Discussion .....	61
4.2.1 Purification and native folding of recombinant hPrP .....	61
4.2.2 hPrP amyloidosis induced by peptide homologs to RF-amide neuropeptides .....	61
4.2.3 hPrP amyloidosis through amyloid seeding.....	69
4.3 Conclusions.....	74
REFERENCES .....	75

## LIST OF TABLES

<b>Table</b>	<b>Page</b>
1.1 Human amyloid proteins and their associated diseases .....	3
3.1 Synthetic peptides tested for the ability to promote amyloidosis of recombinant hPrP.....	43
4.1 RF-amide peptide homologs that were synthesized and tested for the ability to promote amyloidosis of recombinant hPrP.....	62

## LIST OF FIGURES

Figure	Page
1.1 Amyloidosis mechanism.....	5
1.2 Cartoon representation of the native structure of the human prion protein (residues 23-230).....	7
1.3 Peptide effects on PrP <sup>C</sup> to PrP <sup>Sc</sup> conversion .....	9
2.1 Full-length amino acid sequence of the human prion protein.....	14
2.2 IPTG-induced expression of recombinant hPrP in transformed <i>E. coli</i> cells .....	18
2.3 Purification of hPrP from transformed <i>E. coli</i> cells.....	21
2.4 High purity of Ni-NTA isolated recombinant hPrP .....	23
2.5 Specific detection of recombinant hPrP by antibody recognition .....	26
2.6 Proteinase K digestion of recombinant hPrP .....	28
2.7 Fluorescence spectra of Thioflavin T in the presence and absence of amyloid hPrP.....	30
2.8 Fluorescence spectra of natively folded recombinant hPrP and amyloid hPrP .....	31
2.9 Turbidity of natively folded recombinant hPrP relative to amyloid hPrP .....	33
2.10 Far UV-CD spectra of natively folded and amyloid hPrP .....	34
3.1 Far UV-CD spectra of natively folded and peptide-3-induced hPrP amyloid.....	42
3.2 Fluorescence spectra of samples containing hPrP + cyclo-CGGKFAKFGGC, incubated from 0 to 72 hours .....	44
3.3 ThT fluorescence when mixed with hPrP only or the synthetic peptides only.....	46
3.4 Fluorescence spectra of samples containing hPrP + KFAKF or hPrP + cyclo-CGKFAKFGC, and incubated from 0 to 72 hours .....	47

3.5	Fluorescence at 482 nm for quadruplicate samples containing hPrP + cyclo-CGGKFAKFGGC.....	48
3.6	Proteinase K digestion of recombinant hPrP .....	49
3.7	Turbidity of samples containing hPrP + cyclo-CGGKFAKFGGC, incubated from 0 to 72 hours.....	51
3.8	Aggregation of recombinant hPrP .....	53
3.9	PK digestion and ThT fluorescence of samples containing aggregates of hPrP.....	54
3.10	Fluorescence spectra of samples containing hPrP + ~ 100 ng hPrP amyloid, incubated from 0 to 72 hours .....	55
3.11	Turbidity of samples containing hPrP + ~ 100 ng hPrP amyloid, incubated from 0 to 72 hours.....	56
3.12	Fluorescence spectra of samples containing hPrP + 0.1 mM cyclo-CGGKFAKFGGC, incubated from 0 to 72 hours .....	58
4.1	Fluorescence spectra of samples containing hPrP + cyclo-CGGRFMRFGGC, incubated from 0 to 72 hours .....	63
4.2	ThT fluorescence when mixed with hPrP only or the synthetic peptides only.....	65
4.3	Fluorescence spectra of samples containing hPrP + RFMRP or hPrP + cyclo-CGGRFMRFGC, and incubated from 0 to 72 hours.....	66
4.4	Fluorescence at 482 nm for triplicate samples containing hPrP + cyclo-CGGRFMRFGGC .....	67
4.5	Proteinase K digestion recombinant hPrP.....	68
4.6	Turbidity of samples containing hPrP + cyclo-CGGRFMRFGGC, incubated from 0 to 72 hours.....	70
4.7	Fluorescence spectra of samples containing hPrP + ~ 100 ng hPrP amyloid, incubated from 0 to 72 hours .....	71
4.8	Turbidity of samples containing hPrP + ~ 100 ng hPrP amyloid, incubated from 0 to 72 hours.....	72
4.9	Fluorescence spectra of samples containing hPrP + 0.1 mM cyclo-CGGRFMRFGGC, incubated from 0 to 72 hours .....	73

## **ABSTRACT**

**PEPTIDE INDUCED AMYLOIDOSIS OF RECOMBINANT HUMAN**

**PRION PROTEIN**

by

Melody Christine Adam, B.S.

Texas State University-San Marcos

May 2012

**SUPERVISING PROFESSOR: STEVEN WHITTEN**

Protein folding is a process that involves a polypeptide chain folding into a stable and well-defined tertiary structure, which is characteristic of its physiological state and essential for its function. Since protein function is so heavily dependent on its structure, one can visualize that a protein misfolding into a structure other than its normal physiologically-relevant state could present significant problems for the host cell. One type of protein misfolding that is often observed in nature is amyloidosis, which involves the structural conversion of normal protein into amyloid oligomers that are rich in beta structure. These form a plaque of insoluble fibrils that accumulate in organs and tissue. Amyloid oligomers are inherently toxic to neuronal cells and have been implicated in numerous neurodegenerative disorders.

The body of work presented here was initiated to develop a new experimental strategy for identifying molecular interactions that lead to protein amyloidosis. In this pursuit, peptide ligands were designed to bind to the human prion protein and promote prion misfolding into amyloid fibrils. By identifying binding partners that promote or block prion misfolding, important insight into the nature of amyloidosis can be learned. In this thesis, it is shown that a recombinant system was developed for expressing the human prion protein and testing synthetic peptides for their ability to induce prion misfolding. It was also observed that synthetic peptides homologous to the RF-amide class of neuropeptides caused recombinant human prion protein to self-assemble into amyloid fibrils. These results suggest that RF-amide peptides may be physiological cofactors to the prion diseases, demonstrating the potential of this recombinant system for identifying possible disease cofactors, separate from its primary purpose of probing the molecular determinants of protein amyloidosis.

## CHAPTER I

### INTRODUCTION

Numerous human diseases are characterized by the misfolding of cellular protein into insoluble amyloid fibrils.<sup>1</sup> These amyloid fibrils are highly stable and resist protease digestion and cellular clearance<sup>2</sup>, consequently accumulating as plaques in organs and tissues.<sup>3</sup> The buildup of amyloid is cytotoxic to neuronal cells and causes synaptic dysfunction.<sup>4</sup> As a result, most amyloid-related disorders are neurodegenerative and progress through dementia, a loss of control over psychomotor skills, and ultimately death.<sup>5</sup> These diseases occur with greater frequency in older individuals, and are of increasing concern for the aging demographics of industrialized nations.<sup>6</sup> Because of these observations, compounds that interact with amyloid-forming protein are of pharmaceutical interest. The main goal of this project is to test the ability of small peptides to interact with the human prion protein and modulate its conversion to amyloid fibrils. The prion protein has been implicated in many neurodegenerative and fatal amyloidosis disorders, most notably Creutzfeldt-Jakob Disease, Kuru, Fatal Familial Insomnia, and the Transmissible Spongiform Encephalopathies.<sup>7,8</sup>

### ***1.1 Amyloidosis Disorders***

Amyloidosis refers to a class of diseases characterized by the extracellular deposition of insoluble proteinaceous fibrils in organs and tissues.<sup>5</sup> These diseases are differentiated mostly by the particular protein found in the fibrillar deposits.<sup>12</sup> To date, there are approximately 60 different proteins identified in mammals with the ability to form amyloid fibrils.<sup>9</sup> Of these, over 20 human proteins have been associated with amyloid disease.<sup>10</sup> Some of the amyloidosis diseases are inherited and linked to mutations in the gene coding for the associated protein, while others are sporadic, and some transmissible.<sup>11</sup> Among the diseases associated with amyloidosis, these include Alzheimer's disease, Parkinson's disease, Huntington's disease, Transmissible Spongiform Encephalopathy, and Diabetes Mellitus Type II.<sup>12</sup> The accumulation of amyloid deposits in the brain can lead to synaptic alterations, neuronal death, spongiform degeneration, and brain inflammation.<sup>13</sup> Alzheimer's disease, which is the most prevalent neurodegenerative disorder among the elderly, is associated with amyloid deposits that contain beta amyloid (A $\beta$ ).<sup>14</sup> For a list of amyloidogenic proteins and their related diseases, please refer to Table 1.1.

### ***1.2 Structural Models of Amyloid***

Structurally, amyloid fibrils are observed as non-branching rigid protein oligomers, ranging in length from 100 to 1600 nm.<sup>5</sup> The numerous proteins associated with the different amyloid diseases share negligible homology when comparing their amino acid sequences and physiological structures.<sup>2</sup> This contrasts, however, with the amyloid states adopted under diseased conditions, which appear practically identical

**Table 1.1.** Human amyloid proteins and their associated diseases.<sup>16</sup>

---

<b>Associated disease</b>	<b>Protein</b>
Secondary systemic amyloidosis	Serum amyloid protein A
Familial amyloid polyneuropathy Type II	Apolipoprotein A-I
Familial amyloid polyneuropathy Type III	Apolipoprotein A-II
Familial amyloid polyneuropathy Type I	Transthyretin
Corneal amyloidosis	Lactoferrin
Fibrinogen amyloidosis	Fibrinogen
Lysozyme amyloidosis	Lysozyme
Cutaneous amyloidosis	Keratin
Alzheimer's disease, frontotemporal dementia	Tau
Type II diabetes	Amylin
Medullary carcinoma of the thyroid	Calcitonin
Aging pituitary prolactinomas	Prolactin
Insulin-related amyloid	Insulin
Atrial amyloidosis	Atrial natriuretic factor
Finnish hereditary amyloidosis	Gelsolin
Icelandic hereditary cerebral amyloid angiopathy	Cystatin C
Primary systemic amyloidosis, amyloidosis associated with multiple myeloma	Immunoglobulin light chains ( $\kappa$ and $\lambda$ )
Primary systemic amyloidosis	Immunoglobulin heavy chain
Hemodialysis-related amyloidosis	$\beta$ 2-Microglobulin
Corneal dystrophy	Kerato-epithelin
Aortic medial amyloidosis	Lactadherin (Medin)
Alzheimer's disease, cerebral amyloid angiopathy	Amyloid- $\beta$
Spongiform encephalopathies	Prion protein
British familial dementia	Amyloid British
Danish familial dementia	Amyloid Danish
Parkinson's disease	$\alpha$ -Synuclein

---

among the different diseases.<sup>15</sup> This suggests that the various amyloidosis disorders may share common mechanisms and pathways that lead to amyloid misfolding, despite their associations with non-homologous proteins.

Traditional techniques for studying the structures of bio-macromolecules, such as multidimensional nuclear magnetic resonance (NMR) spectroscopy and x-ray crystallography, are of limited application to amyloid fibrils due to their low solubility and polydisperse lengths.<sup>17</sup> Solid-state NMR techniques, however, have been successful at probing the atomic interactions between protein subunits that compose fibrillar structures.<sup>18</sup> These types of studies, and others based on electron microscopy<sup>19</sup>, suggest that amyloid particles are composed of long protofilaments that are approximately 2.7-4.2 nm in diameter.<sup>15</sup> The protofilaments appear to be made of numerous, stacked, curvilinear  $\beta$ -pleated sheets, with the  $\beta$  strands running perpendicular to the fibril axis.<sup>20</sup> And in general, a single amyloid fibril is composed of 3-6 protofilaments.<sup>5</sup>

The mechanism by which proteins misfold into amyloid fibrils is not clearly understood. It has been hypothesized that amyloidosis first proceeds through an initial unfolding of a normal protein into a somewhat compact and loosely structured state, often called the “molten globule” state.<sup>21</sup> These molten globules are thought to be energetically unstable under normal physiological conditions.<sup>22</sup> Chance protein-protein interactions between two or more molten globules, however, could trap the protein in a misfolded, amyloid prone state that would then provide a stable nucleating seed for fibril growth.<sup>23</sup> A schematic representation of this hypothetical self-assembly mechanism to form amyloid fibrils is given in Figure 1.1. Key details about the molecular

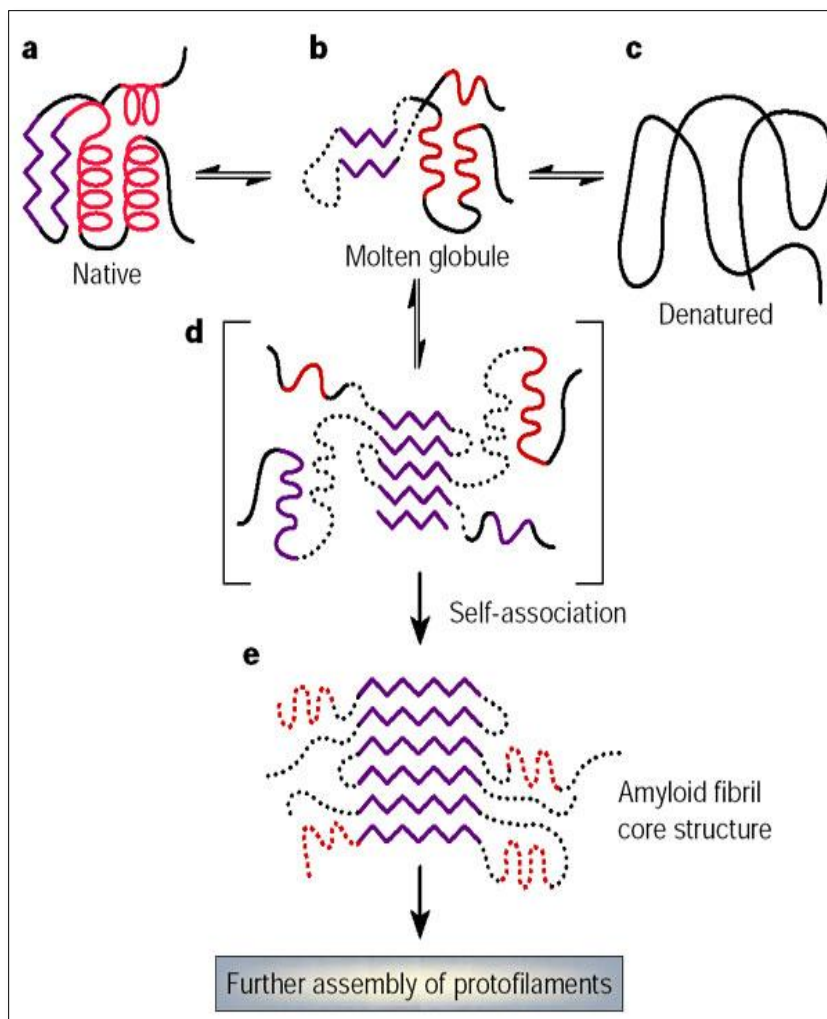


**Figure 1.1. Amyloidosis mechanism.** A proposed mechanism for amyloid misfolding, demonstrating that a loosely folded intermediate may be the precursor to the formation of amyloid fibrils.<sup>21</sup>

interactions that favor amyloid formation and the structural character of the molten globules and misfolded states unfortunately have not yet been determined for any of the proteins implicated in amyloidosis disorders.<sup>24</sup>

### ***1.3 Amyloidosis Induced by Peptide Binding***

Many proteins undergo conformational changes as a result of binding interactions with other molecules.<sup>25</sup> Because amyloidosis involves a conformational change in protein<sup>26</sup>, we decided to try to develop small peptide ligands that could bind to a protein and cause it to self-assemble into amyloid fibrils. Such a system would allow us to investigate the molecular interactions that are salient to amyloid formation. To do this, we took advantage of a recent result demonstrating that binding sites could be distinguished from other regions on the protein surface by their ability to perturb the conformational ensemble, and thus are identifiable based on this property.<sup>27</sup> We decided to attempt this strategy with the prion protein for the following reasons: 1) a high-resolution structure of the prion protein is publically available which we could use with the binding site identification algorithm, and 2) it has been proposed that an unknown protein cofactor, called “Protein X”, interacts with the prion protein to cause amyloid misfolding<sup>28</sup>, suggesting that protein:ligand interactions may indeed be important in the molecular pathology of prion diseases.

Using computer simulation data, a binding site on the C-terminal helix of the human prion protein (hPrP) was identified and a small peptide ligand specific for that site was predicted. The native structure of hPrP is shown in Figure 1.2. Three tyrosine residues (at positions 218, 225, and 226) and two glutamate residues (at positions 211 and

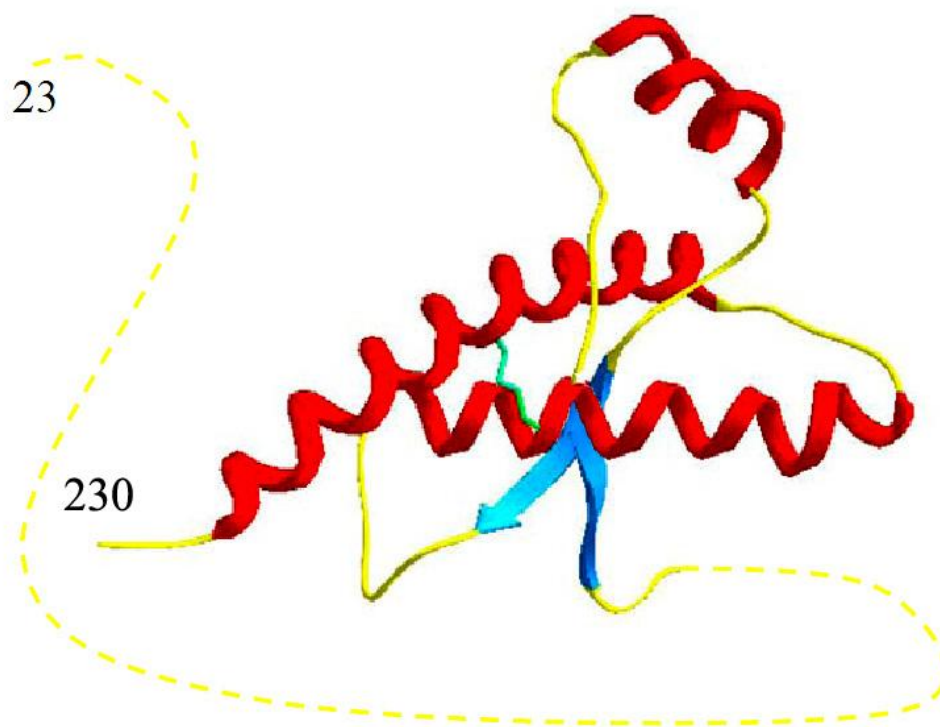


**Figure 1.2. Cartoon representation of the native structure of the human prion protein (residues 23-230).** This cartoon structure was generated from the NMR solution structure solved by Wüthrich and colleagues<sup>29</sup>, and listed in the protein data bank by accession code: 1QLX.

and 219) that are located on the C-terminal helix<sup>29</sup> were used to design a specific, hydrophobic-and-charge-based interaction between hPrP and a peptide ligand with the sequence of KFAKF (lysine-phenylalanine-alanine-lysine-phenylalanine). To minimize unfavorable entropy contributions to the binding energetics, cyclic versions of the KFAKF binding sequence were included in our tests. Structurally constrained ligands, such as cyclic peptides, should have decreased binding entropies, and as a result, increased affinity. In total, three peptides were synthesized commercially, all based upon the KFAKF motif: 1) a short linear peptide consisting of the sequence KFAKF, 2) a small cyclic peptide, cyclo-CGKFAKFGC, and 3) a slightly larger cyclic version, cyclo-CGGKFAKFGGC.

These three peptides were tested initially by Claudio Soto (University of Texas Health Science Center, Houston), using the Protein Misfolding Cyclic Amplification (PMCA) technology that he developed.<sup>30</sup> This method involves obtaining PrP<sup>Sc</sup> (i.e., amyloid PrP, in reference to the “scrapie” isoform<sup>31</sup>) from the brain homogenates of diseased animals and mixing it with native cellular prion protein (PrP<sup>C</sup>) acquired from the brains of healthy animals. This results in the conversion of the normal protein to the misfolded form through a process of seeding that is catalyzed by periodic sonication to create more nucleating seeds. PMCA has been shown to mimic the process of prion replication *in vivo*, resulting in the formation of infectious PrP<sup>Sc</sup><sup>32</sup>, and reproduces the phenomena of prion strains and species barrier<sup>33</sup>, typical of prion diseases. The synthetic peptides were added to a mixture of hamster PrP<sup>C</sup> and PrP<sup>Sc</sup>. As shown in Figure 1.3, PrP<sup>Sc</sup> was not detectable before amplification, since the quantity of misfolded protein added to the mixture was below the limit of detection in the western blot assay. After 124

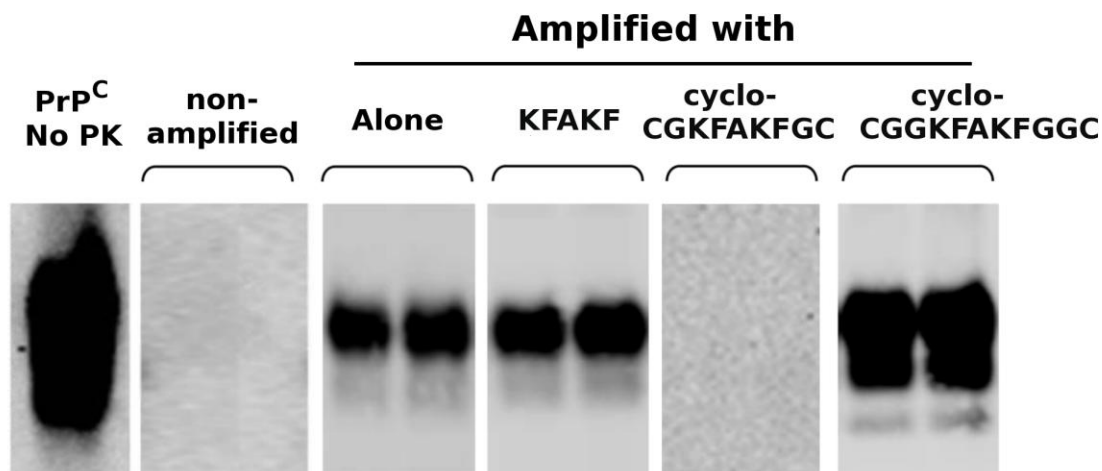


**Figure 1.3. Peptide effects on PrP<sup>C</sup> to PrP<sup>Sc</sup> conversion.** The ability to convert PrP<sup>C</sup> to PrP<sup>Sc</sup> was tested by using the PMCA technology.<sup>32</sup> Here, 400  $\mu$ l samples containing 10 ng PrP<sup>Sc</sup>, 4  $\mu$ g PrP<sup>C</sup>, and 400  $\mu$ g of synthetic peptide were prepared in 1X PBS, 0.1% SDS, 0.1% TritonX-100 and incubated for 62 hours (124 PMCA cycles). Resistance to proteinase K (PK) digestion is used as a marker for PrP<sup>Sc</sup> in this assay; PK digests natively folded PrP<sup>C</sup> but not PrP<sup>Sc</sup>. As controls, shown are PrP<sup>C</sup> without PK digestion (first panel), PrP<sup>C</sup> mixed with PrP<sup>Sc</sup> but not subjected to PMCA (second panel), and the PMCA assay performed with no added peptides (third panel). The fourth, fifth and sixth panels show that the peptide KFAKF had no noticeable effect on PrP<sup>Sc</sup> formation, the peptide cyclo-CGKFAKFGC inhibited PrP<sup>Sc</sup> formation, and the peptide cyclo-CGGKFAKFGGC enhanced PrP<sup>Sc</sup> formation, respectively. The second through sixth panels each show duplicate samples. The western blot protocol employed in the figure is described in section 2.3.3 of this thesis.

PMCA cycles in the absence of peptide, a PrP<sup>Sc</sup> signal was readily detectable, the magnitude of which was not altered by the presence of the KFAKF peptide. In contrast, the shorter cyclic peptide, cyclo-CGKFAKFGC, inhibited the amplification of PrP<sup>Sc</sup>, whereas the longer cyclic peptide, cyclo-CGGKFAKFGGC, enhanced PrP<sup>Sc</sup> formation dramatically.

It is important to recognize that these three synthetic peptides, despite their sequence similarities, each affected the PMCA assay differently. The linear peptide KFAKF obviously didn't interact with PrP, as its presence in the PMCA sample didn't alter the assay results. In contrast, both cyclic peptides apparently interact with PrP (i.e., the presence of either peptide was observed to affect the PMCA results). The binding of the smaller cyclic peptide cyclo-CGKFAKFGC to PrP, however, was unproductive toward PrP<sup>Sc</sup> formation, whereas the binding of the larger cyclic peptide cyclo-CGGKFAKFGGC to PrP was on-pathway, presumably structurally, toward PrP<sup>Sc</sup> conversion and amyloid formation in general. Considering that the PrP:peptide interactions were observed to be sequence dependent, these data suggest that the cyclic peptides bind to PrP, and that slight modifications in those binding interactions can have pronounced structural consequences for PrP, in terms of whether or not amyloid conversion occurs.

#### ***1.4 Research Goals***

The research presented in this thesis involves the development of a recombinant system to test peptide-induced amyloidosis of human prion protein. The results given by Soto suggest that peptides based on the KFAKF sequence may interact with tissue-derived prion protein to modulate the amyloid misfolding of PrP<sup>C</sup> when in the presence of

seeding amounts of PrP<sup>Sc</sup>. For our recombinant studies, the following will be done: 1) express hPrP in a recombinant bacterial system using *Escherichia coli*, 2) purify recombinant hPrP from bacteria and demonstrate that it's correctly folded into its predominantly  $\alpha$ -helical native state, and 3) test the ability of peptides with the sequence of KFAKF, cyclo-CGKFAKFGC, and cyclo-CGGKFAKFGGC to cause amyloid misfolding of natively folded recombinant hPrP. As demonstrated in Chapter 3 (*"Amyloid misfolding of native recombinant human prion protein induced by peptide interactions."*), this research strategy was successful and showed that cyclo-CGGKFAKFGGC interacts with purified recombinant hPrP to promote amyloid misfolding, whereas the other two peptides that were tested did not. These results with recombinant hPrP were consistent with the preliminary results shown in Figure 1.3 that were performed by Soto's group.

The physiological relevance of peptide-induced amyloidosis of the prion protein is at this time unclear. It has been hypothesized by other researchers that a protein-based cofactor interacts with the prion protein to facilitate amyloidosis<sup>34</sup>, however, no protein cofactor has been identified to date. In Chapter 4 of this thesis (*"A peptide homolog to the RF-amide class of neuropeptides induces amyloid misfolding of recombinant human prion protein."*), a second peptide set was tested for the ability to promote hPrP amyloidosis. The sequences of these peptides were based on the FMRF sequence of a short neuropeptide that was initially isolated in clams, but later found to have mammalian homologs.<sup>35</sup> The peptide sequences tested in Chapter 4 were RFMRF, cyclo-CGRFMRFGC, and cyclo-CGGRFMRFGGC, and thus homologous to the KFAKF-based peptides. It was observed that the larger cyclic peptide, cyclo-CGGRFMRFGGC,

caused amyloid misfolding of recombinant hPrP, similar to what was observed with cyclo-CGGKFAKFGGC.

## CHAPTER II

### MATERIALS AND METHODS

#### 2.1 *Materials*

All chemicals and reagents used for this project were Molecular Biology grade or higher. Synthetic peptides were synthesized commercially to 98% purity by GenScript (Piscataway, NJ) and Peptide 2.0 (Chantilly, VA). Water used in sample preparation was filtered and deionized by a Millipore Milli-Q purification unit (Billerica, MA). Prior to use, all glassware, pipette tips, and micro-centrifuge tubes were sterilized with a HICLAVE HV-50 autoclave vessel by Hirayama (Westbury, NY).

#### 2.2 *Cloning, Over-Expression, and Purification of Recombinant Human Prion Protein*

##### 2.2.1 *Cloning and transformation of bacterial cell cultures*

A gene coding for residues 23-230 of hPrP was cloned into a plasmid expression vector by DNA 2.0 (Menlo Park, California). Figure 2.1 shows the amino acid sequence used in our studies, and represents the consensus wild type hPrP sequence.<sup>36</sup> Codon usage for this gene was optimized for protein expression in *Echerichia coli* cells using an

```
1  manlgcwmlv lfvatwsdlg lckkrpkpgg wntggsrypg qgspggnryp pgggggwgqp  
61  hgggwgqphg ggwgqphggg wqphggggwg qgggthsqwn kpskpktnmk hmagaaaaga  
121 vvgglggyvl gsamsrpiih fgdyedryy renmhrypna vyyrpmdeys nqnnfvhdcv  
181 nitikqhtvt tttkgenfte tdvkmmervv eqmcitqyer esqayykrqs smvlfssppv  
241 illisflifl ivg
```

**Figure 2.1. Full-length amino acid sequence of the human prion protein.** Residues 1-22 constitute a signal peptide that directs the prion protein for synthesis via the secretory pathway and is removed during translation.<sup>13</sup> The prion protein is initially anchored to the external cell-surface by a glycosylphosphatidylinositol (GPI) linker.<sup>37</sup> The mature form of hPrP is free of the GPI anchor and consists of residues 23-230. All studies herein used the mature form of hPrP consisting of residues 23-230.

algorithm developed by DNA 2.0.<sup>38</sup> A pJexpress bacterial plasmid vector (pJexpress404) was used that had the T5 promoter sequence to allow isopropyl  $\beta$ -D-1-thiogalactopyranoside (IPTG)-induced expression of hPrP in any *E. coli* host.<sup>39</sup> The pJexpress plasmid also contained a high-copy-number pUC origin of replication (~150-200 copies/cell), and an ampicillin resistance gene (*ampR*) to express the enzyme beta-lactamase and neutralize antibiotics in the penicillin group. Upon receipt from DNA 2.0, plasmids containing the hPrP gene were solubilized in DNA grade sterile water to a concentration of 1 ng/ $\mu$ L and stored in sterile cryovial tubes at -80°C.

BL21 (DE3) pLysS competent cells by Novagen (Darmstadt, Germany) were transformed by adding 7 $\mu$ L of plasmid stock to 50  $\mu$ L of competent cells suspended in 60 mM calcium chloride. The gently mixed sample of cells and plasmid was placed on ice for 5 minutes, then in a heat bath (42°C) for 30 seconds, and then on ice again for 2 minutes. Next, a volume of 250  $\mu$ L Super Optimal Broth with Catabolite repression (SOC) was added at room temperature. Approximately 150  $\mu$ L of the cell culture was then propagated on lysogeny broth (LB) agarose plates containing 100  $\mu$ g/mL of ampicillin to select for transformed *E. coli* cells.

### 2.2.2 Glycerol stocks of transformed *E. coli* cells for long term storage at -80°C

An Erlenmeyer flask containing 200 mL of LB and 100  $\mu$ g/mL of ampicillin was aseptically inoculated with a single colony of *E. coli* cells transformed with plasmid containing the hPrP gene as described above. The 200 mL cell culture was incubated overnight in a rotary incubator (Max\*Q, MIDSCI, St. Louis, MO) at 30°C with orbital rotation. The next morning, 5 mL of cell culture was transferred to 200 mL of fresh LB

with 100 µg/mL ampicillin and incubated with orbital rotation at 37°C to an optical density (OD) of 0.6 at 600 nm. At this point, 800 µL of cell culture was mixed with 200 µL of sterile 80% glycerol. Glycerol stocks containing transformed cell cultures were stored in sterile cryovial tubes at -80°C.

### 2.2.3 *Bacterial over-expression of recombinant hPrP*

For bacterial growth and induction of protein, first an aseptic dab of *E. coli* from a glycerol stock was spread onto an LB agar plate containing 100 µg/mL of ampicillin. The plate was then incubated at 37°C overnight or until single colonies grew to a reasonable size (~1 mm diameter). Next, a single colony grown on the agar plate was used to inoculate 10 mL of sterile LB + 100 µg/mL ampicillin. The inoculated sample was incubated with orbital rotation at 37°C until visibly turbid (~ 3-4 hours). Then, 2.5 mL of the inoculated sample was transferred into each of 4 flasks containing 250 mL of fresh sterile LB + amp. The 4 flasks were incubated with orbital rotation at 37°C until an OD of 0.6 was measured at 600 nm, at which point IPTG was added to a concentration of 0.5 mM to induce hPrP expression. The cell cultures were incubated for an additional 4 hours at 37°C with orbital rotation, and then harvested by centrifugation at 7,000 RPM, 4°C, for 20 minutes, using a Beckman J2-21 centrifuge with a JA-14 rotor. The supernatant was poured off and cell pellets were stored overnight at -20°C for hPrP purification from cell lysate the next day.

Sodium dodecyl sulfate polyacrylamide gel electrophoresis (SDS-PAGE) was used to verify IPTG-induced expression of hPrP in transformed *E. coli* cells. This is

shown in Figure 2.2. Briefly, cell cultures grown from multiple glycerol stocks were lysed and electrophoresed pre- and post-induction. As is clear from the figure, a protein with the molecular weight of approximately 23 kDa, which is similar to the molecular weight of hPrP (22.86 kDa; determined by its sequence), was expressed in the transformed cells only when IPTG was added. Details of the SDS-PAGE protocol are given in section 2.3.1. Western blots using antibodies specific to hPrP were also used to verify hPrP expression in the transformed *E. coli* cells (see Figure 2.5 and section 2.3.3).

#### 2.2.4 Purification of recombinant hPrP from *E. coli* cells

Frozen cell pellets containing hPrP were thawed and suspended in 20 mL of lysis buffer (10 mM Tris-HCl, 2 mM EDTA, 100 mM NaCl, 100 µg/mL lysozyme, pH 7.5). The suspension was then incubated for 30 minutes at 37°C to allow lysozyme to weaken the bacterial cell wall. Next, the cells were sonicated using a Bronson Sonifier S-450A (Danbury, CT). The sample was kept on ice during sonication to preventing excessive heating. The sonication procedure consisted of three 1-minute pulses separated by 1-minute rest periods. The sonifier was set to a duty cycle of 80% and half-maximum output (control set to 5).

Following sonication, TritonX-100 was added to a final concentration of 1% and the sample was centrifuged at 25,000xg, 4°C, for 45 minutes. Over-expression of hPrP in *E. coli* cells caused the protein to accumulate in inclusion bodies. Thus, following centrifugation of the cell lysate, hPrP was found in the pellet and the supernatant was discarded. The protein pellet was then dissolved in 10 mL of resuspension buffer (8 M urea, 20 mM Tris-HCl, 100 mM NaCl, pH 8.0) and chilled overnight at 4°C.

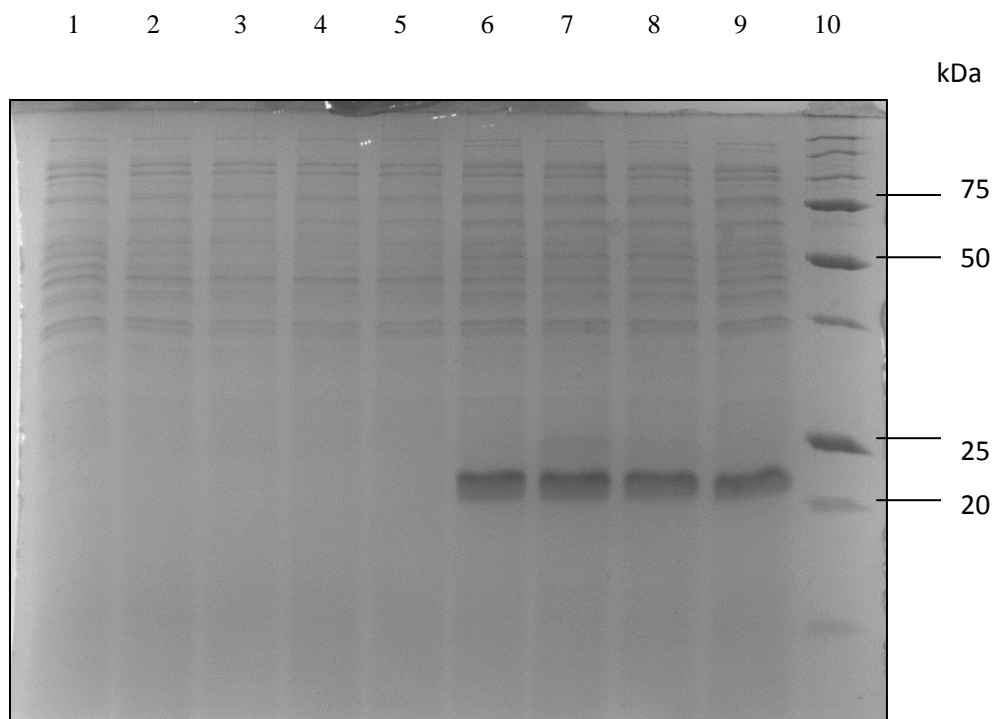


**Figure 2.2. IPTG-induced expression of recombinant hPrP in transformed *E. coli* cells.** Cell cultures derived from 5 glycerol stocks were grown in LB + 100  $\mu\text{g}/\text{mL}$  ampicillin to an OD of 0.6 at 600 nm. To induce protein expression, 0.5 mM IPTG was then added to each culture. Samples taken from each cell culture prior to the addition of IPTG were lysed by boiling for 5 minutes and then ran in lanes 1-5. Samples from the cell cultures taken 4 hours post-induction were similarly lysed and then ran in lanes 6-9. The sample containing glycerol stock #5 post-induction was omitted from the experiment to provide a lane for molecular weight standards. The sizes of some of the molecular weight standards are given in the figure.

The following morning, the protein solution was centrifuged at 10,000xg, 4°C, for 20 minutes. Any observed pellet was discarded and the supernatant was loaded onto a nickel(II)-nitriloacetate (Ni-NTA) column for purification by affinity chromatography. hPrP has a natural affinity for Ni-NTA agarose resin and doesn't require a 6x-Histidine tag.<sup>40</sup>

Purification of hPrP from Ni-NTA resin used a BioLogic LP system from Bio-Rad Laboratories (Hercules, CA). In brief, the Ni-NTA resin was rinsed in-column with 30 mL of dH<sub>2</sub>O to wash out the storage solution (20% ethanol). Next, the column was equilibrated with 30 mL equilibration buffer (8 M urea, 20 mM Tris-HCl, 100 mM NaCl, pH 8.0), after which the hPrP protein sample was carefully loaded onto the column. The column was then washed with 30 mL of wash buffer A (20 mM Tris-HCl, 100 mM NaCl, 8 M urea, pH 8.0), followed by 30 mL of wash buffer B (20 mM Tris-HCl, 100 mM NaCl, pH 8.0), and 30 mL of wash buffer C (20 mM Na<sub>2</sub>HPO<sub>4</sub>, 100 mM NaCl, pH 8.0). After the column wash, hPrP was eluted using a drop in solution pH and the addition of imidazole. The elution buffer consisted of 20 mM Na<sub>2</sub>HPO<sub>4</sub>, 100 mM NaCl, 500 mM imidazole, pH 4.5.

Lastly, the eluted protein was consecutively dialyzed against dialysis buffer A (10 mM Na<sub>2</sub>HPO<sub>4</sub>, pH 5.8) and dialysis buffer B (5 mM Tris-HCl, pH 8.5) at 4°C for a minimum of 4 hours each. The purification of hPrP from cell lysate is shown in Figure 2.3, as followed by gel electrophoresis applied to samples taken at various steps in the purification protocol. The purity of the final hPrP sample was judged to be >99% by silver staining and is shown in Figure 2.4.

## 2.3 *Protein Detection Methods*

### 2.3.1 *Sodium dodecyl sulfate polyacrylamide gel electrophoresis (SDS PAGE)*

SDS-PAGE is commonly used to detect proteins based on their molecular weight.<sup>18</sup> The denaturing conditions used by this technique cause proteins to separate electrophoretically according to the lengths of their polypeptide chains, with very few exceptions (e.g., proteins rich in proline). Shown in Figure 2.3 are results from SDS-PAGE applied to samples taken at various steps in the purification of hPrP.

For optimal separation of proteins in the 10-100 kDa range using SDS-PAGE, first a 15% polyacrylamide gel was made. This was accomplished by initially mixing a 30% acrylamide/bis solution (87.6 g acrylamide, 2.4 g N'-N'bis-methylene-acrylamide, dH<sub>2</sub>O to 100 mL), where acrylamide acts as the polymer and bis-acrylamide as the crosslinker. Next, 5.0 mL of 30% acrylamide/bis solution was added to 5 mL of buffer (2.4 mL dH<sub>2</sub>O, 2.5 mL 1.5 M Tris-HCl (pH 8.8), 100 µL 10% SDS) to make a 15% resolving gel solution. To catalyze the polymerization reaction, 50 µL of 10 % Ammonium Persulfate (APS), which provides free radicals to induce polymerization, and 5 µL of Tetramethyl-ethylenediamine (TEMED), which promotes the formation of APS free radicals, was added to the gel solution. A glass Pasteur pipet was used to quickly transfer this gel solution to a casting stand between two glass plates. The gel was immediately layered with dH<sub>2</sub>O to prevent drying during polymerization. Approximately 45 minutes was allowed for complete polymerization, and then the overlay water was decanted off. A 4% stacking gel buffer (3.05 mL dH<sub>2</sub>O, 650 µL 30% acrylamide/bis, 1.25 mL 0.5 M Tris-HCl (pH 6.8), 50 µL 10% SDS), including 25 µL of 10% APS and 5 µL

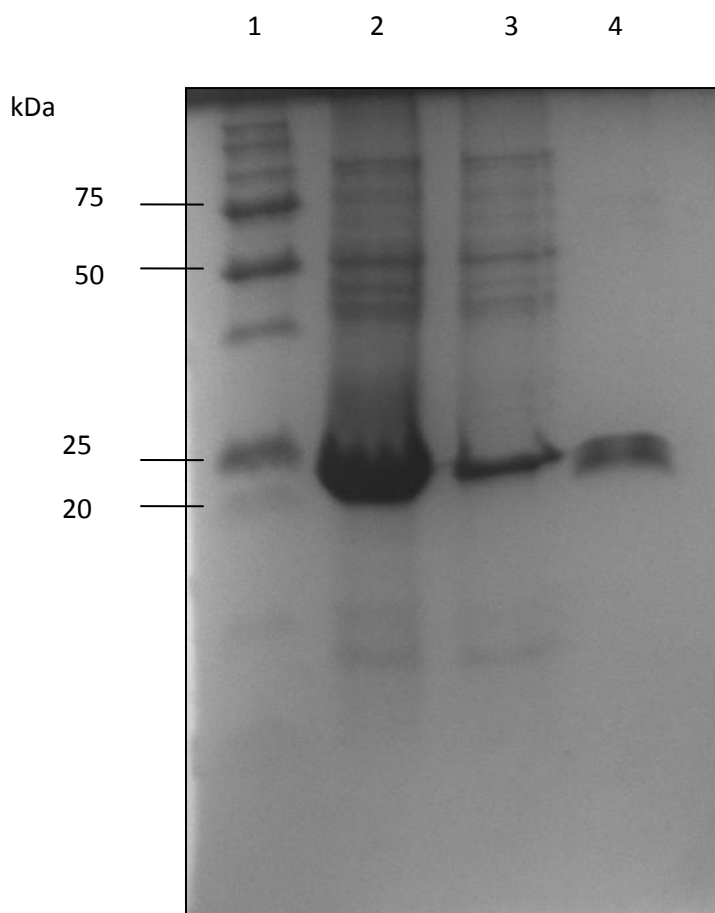


**Figure 2.3. Purification of hPrP from transformed *E. coli* cells.** SDS-PAGE was used to follow the progress of hPrP throughout its purification. Shown in lane 1 are molecular weight standards with their sizes as indicated. Lane 2 shows the proteins that were observed in the insoluble fraction of the cell lysate (i.e., proteins in inclusion bodies). These proteins were solubilized by 8 M urea and then loaded onto the Ni-NTA column for hPrP isolation. hPrP has a molecular weight of 23 kDa and is apparent in the gel as the dominant dark band of lane 2. Lane 3 shows the proteins that eluted from the Ni-NTA column during the column wash. Lane 4 shows the proteins that eluted from the column from the drop in solution pH to 4.5 and the addition of 500 mM imidazole.

of TEMED to catalyze cross-linking, was poured over the resolving gel. Finally, combs were inserted and the gel was allowed to polymerize for an additional 45 minutes. After this time, the gel was ready for use.

After the 15% polyacrylamide gel was prepared, 10  $\mu$ L of sample was mixed with 10  $\mu$ L of 2X Laemmli buffer (100 mM Tris-HCl, 30% glycerol, 4% SDS, 0.02% bromophenol blue, 200 mM DTT), and then boiled for 5 minutes to completely denature any proteins present in the sample. Each sample was then loaded onto individual gel lanes and electrophoresed for 10 minutes at 100 V (constant voltage), followed by 200 V (constant voltage) for 45 minutes. The tank buffer used during electrophoresis was 25 mM Tris, 192 mM glycine, 0.1% SDS, pH 8.3. All electrophoresis experiments used a Bio-Rad Mini PROTEAN Tetra Cell electrophoresis module and a Power Pac Universal Power Supply, both purchased from Bio-Rad Laboratories (Hercules, CA).

Following electrophoresis, most gels were stained using a Coomassie-based method. In brief, a gel was soaked in a Coomassie staining solution for 45 minutes and then soaked for 2-4 hours in a destaining solution. The Coomassie staining solution was made by mixing 1.25 g Coomassie brilliant blue R 250, 227 mL of methanol, 46 mL of glacial acetic acid, and dH<sub>2</sub>O to 500 mL. The destaining solution was made by mixing 200 mL of methanol, 65.5 mL of glacial acetic acid, and dH<sub>2</sub>O to 1 liter.

### 2.3.2 *Silver nitrate staining of polyacrylamide electrophoresis gels*

Silver staining can be used to detect proteins in a polyacrylamide gel at sensitivities as low as single nanogram amounts, and thus can be used to gauge the purity of protein samples.<sup>41</sup> Shown in Figure 2.4 are the results of silver staining a gel of

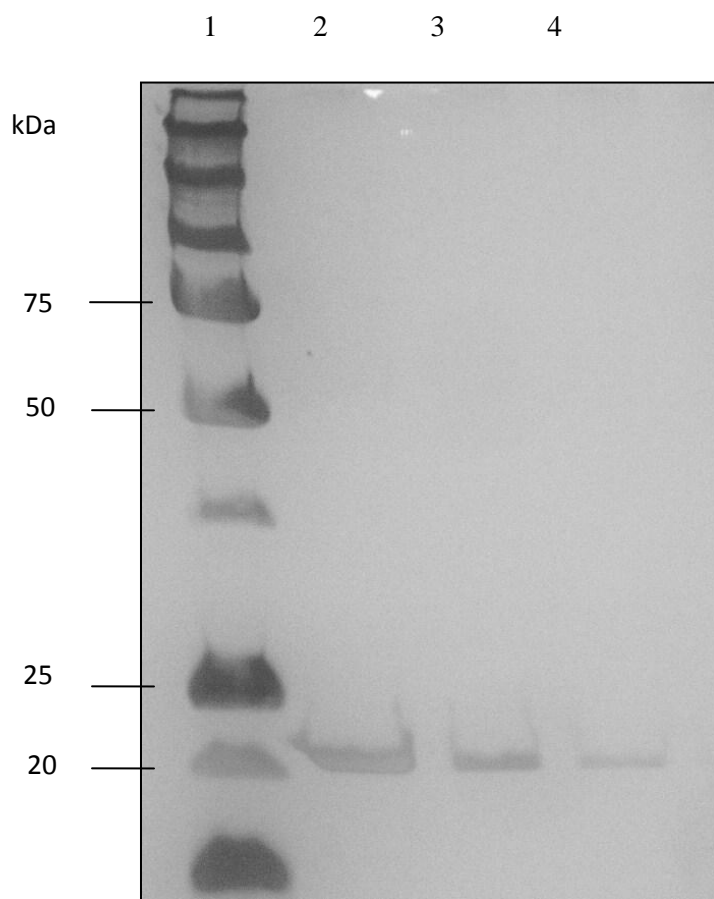


**Figure 2.4. High purity of Ni-NTA isolated recombinant hPrP.** Samples of hPrP purified by Ni<sup>2+</sup> affinity chromatography were gel electrophoresed using standard SDS-PAGE methods and stained with silver nitrate. Shown in lane 1 are molecular weight standards with their sizes as indicated. Lanes 2-5 show purified hPrP at the following concentrations; lane 2 = 19  $\mu$ M; lane 3 = 9.5  $\mu$ M; and lane 4 = 4.75  $\mu$ M. No contaminating bands were visible in the silver stained gel, suggesting that hPrP was highly purified (>99%).

recombinant hPrP purified by the protocol outlined in section 2.2.4 and electrophoresed using the SDS-PAGE methods given in section 2.3.1. No contaminating bands were observed at the highest concentration of hPrP tested (19  $\mu\text{M}$ ), suggesting that the purity of hPrP in that sample was greater than 99%, which was typical in our experiments. The sample volume used in each lane was 10  $\mu\text{L}$ , which would indicate that approximately 4  $\mu\text{g}$  of hPrP was loaded onto the gel in lane 2. Considering the nanogram sensitivity of silver staining, these data demonstrate that any protein contaminants should be at amounts no greater than 1/1000<sup>th</sup> the gram-amount of hPrP.

The silver staining of protein in polyacrylamide gels used the following procedure: First the gel was soaked for 30 minutes in a fixer solution at room temperature and with gentle rocking (e.g., orbital rotation). The role of the fixer was to wash out compounds that may interfere with the silver stain and to crosslink protein macromolecules and limit their diffusion. The fixer was made from 250 mL methanol, 60 mL glacial acetic acid, 0.125 mL of 37.5% formaldehyde, and dH<sub>2</sub>O to 500 mL. Next, the gel was rinsed twice in 50% ethanol for 15 minutes, and then treated for 1 minute with 5 mM sodium thiosulfate to increase the sensitivity of the proteins in the gel for silver ions. Afterwards, the gel was rinsed 3 times with dH<sub>2</sub>O for 20 seconds each, and then soaked for 20 minutes at 4°C in 12 mM AgNO<sub>3</sub> and 0.02% formaldehyde to permeate the gel with silver ions. Lastly, the gel was soaked in 150 mL of a reducing buffer (300 mM sodium carbonate, 0.15 mM sodium thiosulfate, 0.02% formaldehyde) for 10 seconds to reduce the silver ions to metallic silver. An additional wash in fresh reducing buffer for approximately 1 minute was used to increase the silver intensity in protein bands.

### 2.3.3 *Western Blot detection of hPrP*

The presence of hPrP in a sample was detected using the mouse monoclonal antibody 3F4 (Covance, Princeton, NJ) and a standard Western blot technique. Representative results are shown in Figure 2.5. The 3F4 antibody binds to residues 109-112 of hPrP. Protein macromolecules in a sample were first separated using standard SDS-PAGE (see section 2.3.1) and then blot-transferred to a nitrocellulose membrane using a Criterion Blotter from Bio-Rad Laboratories (Hercules, CA). The blot-transfer was for 30 minutes, 100 V, 4°C, and used Towbin's electrotransfer buffer (25 mM Trizma, 192 mM Glycine, 20% w/v methanol, pH 8.3). After transfer, the membrane was soaked overnight at 4°C with orbital rotation in a solution of 5% non-fat dry milk in Tris-Tween buffered saline (20 mM Trizma, 0.1 M NaCl, 0.1% w/v Tween-20, pH 7.5). The following morning, the membrane was incubated for 1 hour with fresh milk + Tris-Tween buffered saline and the 3F4 antibody diluted 1:1000 relative to the stock solution provided by Covance. Next, the membrane was washed three times in 50 mL of fresh milk + Tris-Tween buffer saline for 10 minutes each and then incubated for 1 hour at room temperature with an anti-mouse IgG conjugated to horseradish peroxidase (GE Healthcare, Piscataway, NJ). The anti-mouse IgG was diluted 1:40,000 in fresh milk + Tris-Tween saline. The anti-mouse IgG binds to the 3F4 antibody and was detected using an ECL Plus chemiluminescence kit from GE Healthcare, and imaged with a FOTO/Analyst FX imager from Fotodyne, Inc. (Hartland, WI).

### 2.3.4 *Estimating hPrP concentration by absorbance spectroscopy at 280 nm*

The concentration of the protein was determined by the absorbance of the sample

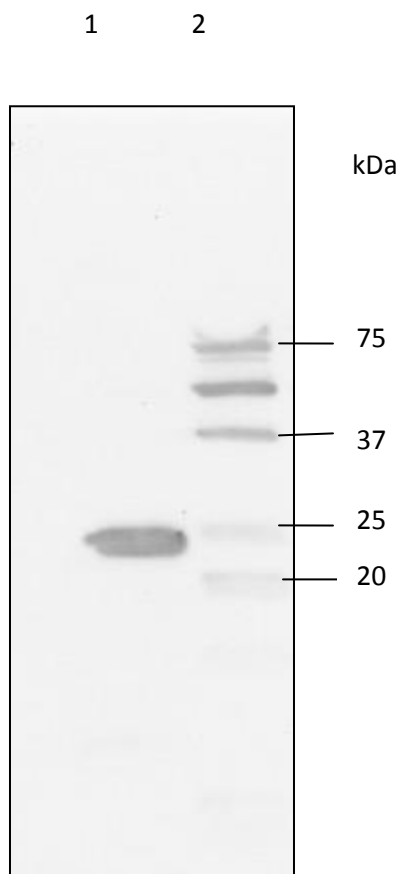


**Figure 2.5. Specific detection of recombinant hPrP by antibody recognition.**

Standard western blot techniques were used to detect the presence of hPrP in protein samples using the monoclonal mouse antibody 3F4(Covance, Princeton, NJ). Shown in lane 1 is 15  $\mu$ M hPrP, purified by nickel affinity from chemically competent *E. coli* cells transformed with plasmid coding for the hPrP gene. Shown in lane 2 are molecular weight standards with their sizes as indicated. The standards each contain a Strep-tag (Strep-tag Western C Protein Standards, Bio-Rad Laboratories, Hercules, CA) for detection by horseradish peroxidase conjugated to Strep-Tactin, rather than antibody affinity.

at 280 nm, using an extinction coefficient of  $57870 \text{ M}^{-1} \text{ cm}^{-1}$ . The extinction coefficient for hPrP was estimated from its amino acid sequence.<sup>42</sup> The Beer-Lambert law was used to convert measured absorbance to protein concentration by:

$$A = \epsilon cl, \quad (2.1)$$

where  $A$  was the measured absorbance,  $\epsilon$  the extinction coefficient,  $c$  the protein concentration, and  $l$  the cuvette width.

## 2.4 *Amyloid Detection Methods*

### 2.4.1 *Detecting amyloid by resistance to Proteinase K digestion*

Native, cellular prion protein (i.e., PrP<sup>c</sup>) is monomeric, soluble under normal aqueous conditions, and readily hydrolyzed by proteases.<sup>7</sup> Amyloid prions (e.g., PrP<sup>S<sup>c</sup></sup>), on the other hand, are insoluble and partially resistant to enzymatic digestion.<sup>32</sup> Thus, an observed resistance to digestion by the protease Proteinase K (PK) has been used to detect the presence of amyloid particles in sample solutions.<sup>43</sup> An example of this detection method is demonstrated in Figure 2.6. This protocol consists of 19  $\mu\text{L}$  of an hPrP sample being mixed with 1  $\mu\text{L}$  of stock PK (stored at 10  $\mu\text{g}/\text{mL}$ ) and incubated at 37°C for 1 hour in an Eppendorf Thermomixer R (Hauppauge, NY). The reaction was quenched by adding 30  $\mu\text{L}$  of 2X Laemmli Sample Buffer (62.5 mM Tris-HCl, 25% Glycerol, 2% SDS, 0.01% Bromophenol Blue, pH 6.8), and boiling at 100°C for 10 minutes. Protein fragments in the sample were then separated by SDS-PAGE (section 2.3.1) and imaged by western blot (section 2.3.3). Natively folded hPrP is digested by PK into very small fragments and passes through the gel during electrophoretic separation.<sup>7</sup>

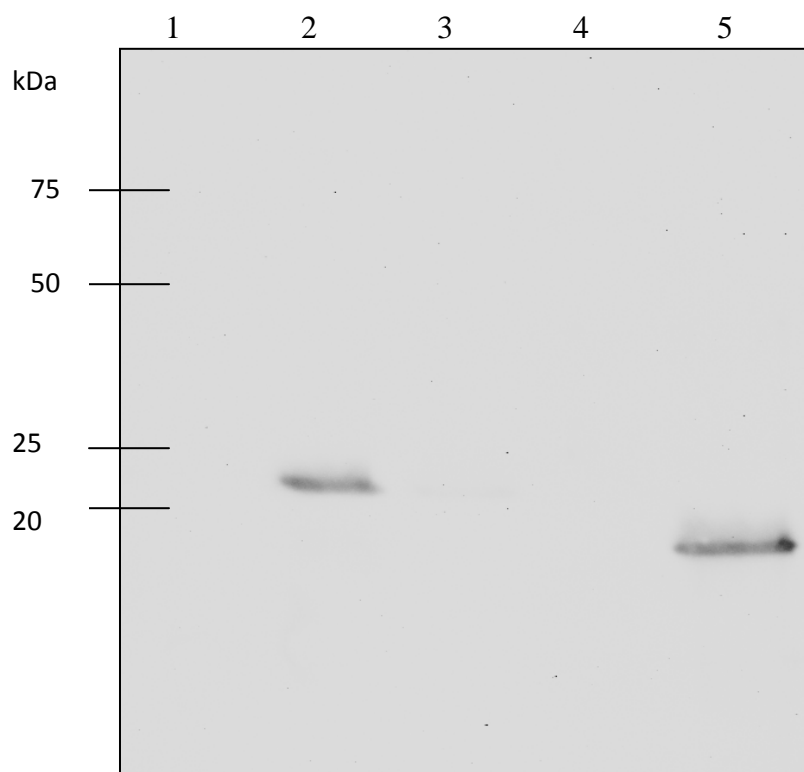


**Figure 2.6. Proteinase K digestion of recombinant hPrP.** Western blot profile showing protease resistance of amyloid hPrP, using the monoclonal antibody 3F4. Shown in lane 1 is 11  $\mu$ M hPrP plus 10  $\mu$ g/mL PK, incubated at 37°C for 1 hr. Shown in lane 2 is 11  $\mu$ M hPrP, without the addition of PK. Lanes 3-5 show additional hPrP samples, but only the sample electrophoresed in lane 5 contained amyloid hPrP, as evidenced by the 16 kDa protease resistant core. After completion of immunoblotting, the polyacrylamide gel was stained with coomassie to view molecular weight standards that were electrophoresed in an additional lane and estimate their positions in the gel image.

The limited proteolysis of PrP<sup>Sc</sup> produces a peptide with a molecular weight ranging from 27 to 30 kDa (depending on glycosylation state) by digesting 67 amino acids off the N-terminal tail. This protease resistant core consists of residues 90-230 and is referred to as PrP 27-30.<sup>44</sup> In the absence of glycosylation, the protease resistant core is observed as a 16 kDa fragment<sup>33</sup>, which can also be estimated from the sequence of residues 90-230 (16.03 kDa).

#### 2.4.2 *Detecting amyloid by Thioflavin T fluorescence*

Thioflavin T is a benzothiazole dye that is commonly used to detect and quantify amyloid in a sample, due to a characteristic shift in its fluorescence spectra when the dye binds to amyloid particles.<sup>45</sup> Shown in Figure 2.7 is the fluorescence shift observed in Thioflavin T as caused by binding interactions with hPrP amyloid. To detect amyloid in a sample, 15  $\mu$ L of the protein sample was mixed with 985  $\mu$ L of 10  $\mu$ M Thioflavin T, 50 mM glycine, pH 8.5. The sample fluorescence was then measured at room temperature using a 1 cm quartz cuvette and a Varian Cary Eclipse fluorescence spectrophotometer (Santa Clara, CA). The emission fluorescence of the sample was measured from 450 nm to 600 nm, due to excitation at 442 nm. Representative data are shown in Figure 2.8. All Thioflavin T solutions were made fresh, directly before use, and protected from sunlight by wrapping the solution container in aluminum foil. Thioflavin T solutions aged more than 3 hours gave inconsistent fluorescence readings in our trials.

#### 2.4.3 *Detecting amyloid by light scattering at 400 nm*

Aqueous solutions containing amyloid particles are visibly turbid and scatter light readily at 400 nm.<sup>48</sup> The ability of aqueous solutions to scatter light, as measured by

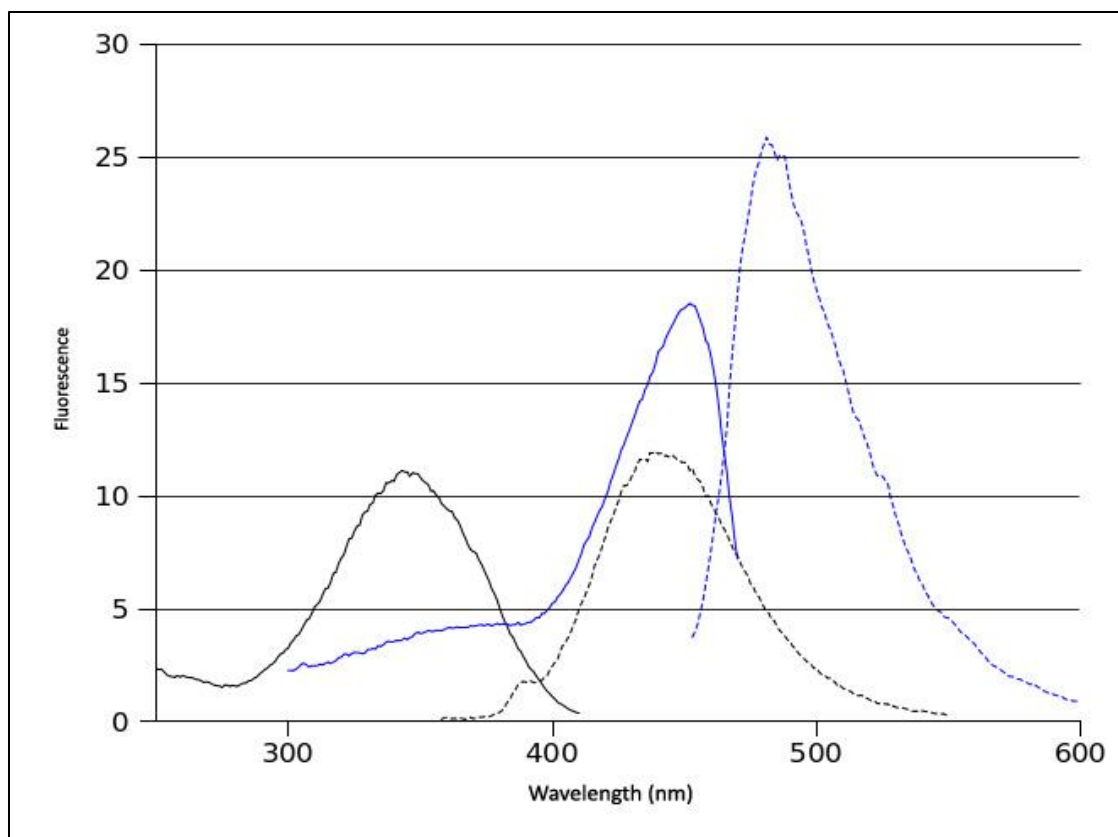


**Figure 2.7. Fluorescence spectra of Thioflavin T in the presence and absence of amyloid hPrP.** The black solid line is the excitation spectrum of 10  $\mu\text{M}$  ThT when the sample was excited at 430 nm (i.e.,  $\lambda_{\text{em}} = 430$  nm). The black dotted line is the emission spectrum of 10  $\mu\text{M}$  ThT ( $\lambda_{\text{ex}} = 342$  nm). The blue solid line is the excitation spectrum of 10  $\mu\text{M}$  ThT + amyloid hPrP ( $\lambda_{\text{em}} = 482$  nm). The blue dotted line is the emission spectrum of 10  $\mu\text{M}$  ThT +  $\sim 5$   $\mu\text{g}$  of amyloid hPrP ( $\lambda_{\text{ex}} = 442$  nm).

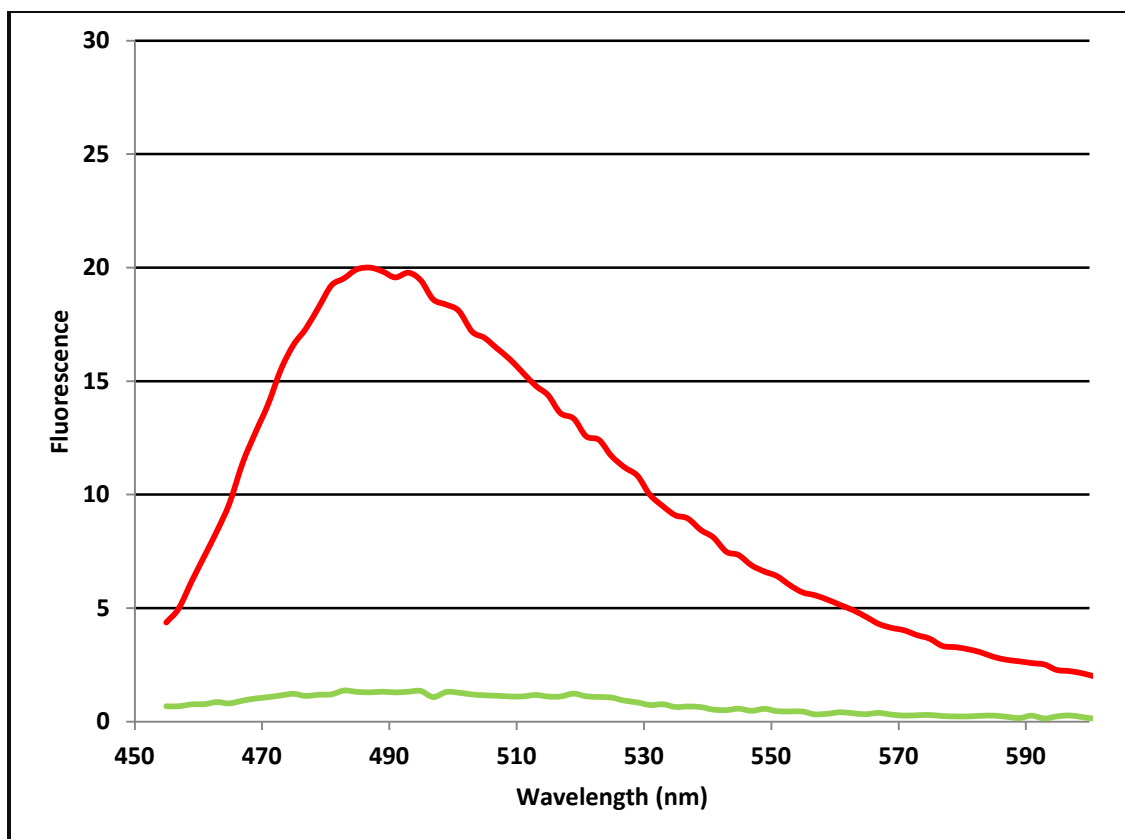


**Figure 2.8. Fluorescence spectra of natively folded recombinant hPrP and amyloid hPrP.** For each sample, its emission spectrum was measured from 460 nm to 600 nm while using an excitation wavelength of 442 nm. The green line represents 985  $\mu\text{L}$  ThT solution (10  $\mu\text{M}$  ThT, 50 mM glycine, pH 8.5) mixed with 15  $\mu\text{L}$  of 11.5  $\mu\text{M}$  hPrP. The red line represents 985  $\mu\text{L}$  ThT solution + 15  $\mu\text{L}$  of a sample estimated to contain 0.5 mg/mL amyloid hPrP.

sample absorbance at 400 nm, has thus been used to detect and quantify amyloid content.

Representative data of this method are provided in Figure 2.9. To detect amyloid in a sample, the absorbance of 80  $\mu$ L of an hPrP sample was measured at 400 nm using a Beckman Coulter DU 730 spectrophotometer (Fullerton, California) and subtracting out an appropriate blank. A 1 cm quartz micro-cuvette was used for all turbidity measurements.

#### 2.4.4 *Detecting amyloid by circular dichroism spectropolarimetry*

Circular dichroism (CD) spectroscopy is used extensively in protein structural studies because of its ability to distinguish between  $\alpha$  helical and  $\beta$  sheet conformations.<sup>46</sup> The native, cellular form of the prion protein (PrP<sup>C</sup>) is predominantly  $\alpha$  helical in structure, consisting of 3 large helices that span residues 144-154, 173-194, and 200-228, and a very small  $\beta$  sheet that maps to residues 128-131 and 161-164.<sup>46</sup> In contrast, amyloid particles are  $\beta$  sheet rich.<sup>47</sup> Thus, by measuring the CD spectrum of hPrP, this  $\alpha$ -to- $\beta$  conformational change can be followed. Representative data for this method are given in Figure 2.10. The CD spectrum of native hPrP displays the characteristic minima at 208 nm and 222 nm that is a hallmark signature of  $\alpha$  helical structures.<sup>47</sup> The CD spectrum of amyloid hPrP, however, shows a negative minimum near 218 nm and a positive maximum at 196 nm, which are associated with  $\beta$  sheets.<sup>12</sup> The far UV-CD spectra of both natively folded and amyloid hPrP is provided in Figure 2.10.

The CD spectrum of each sample was measured using a Jasco J-710 spectropolarimeter (Easton, MD) while purging the optical housing with N<sub>2</sub> gas at a flow

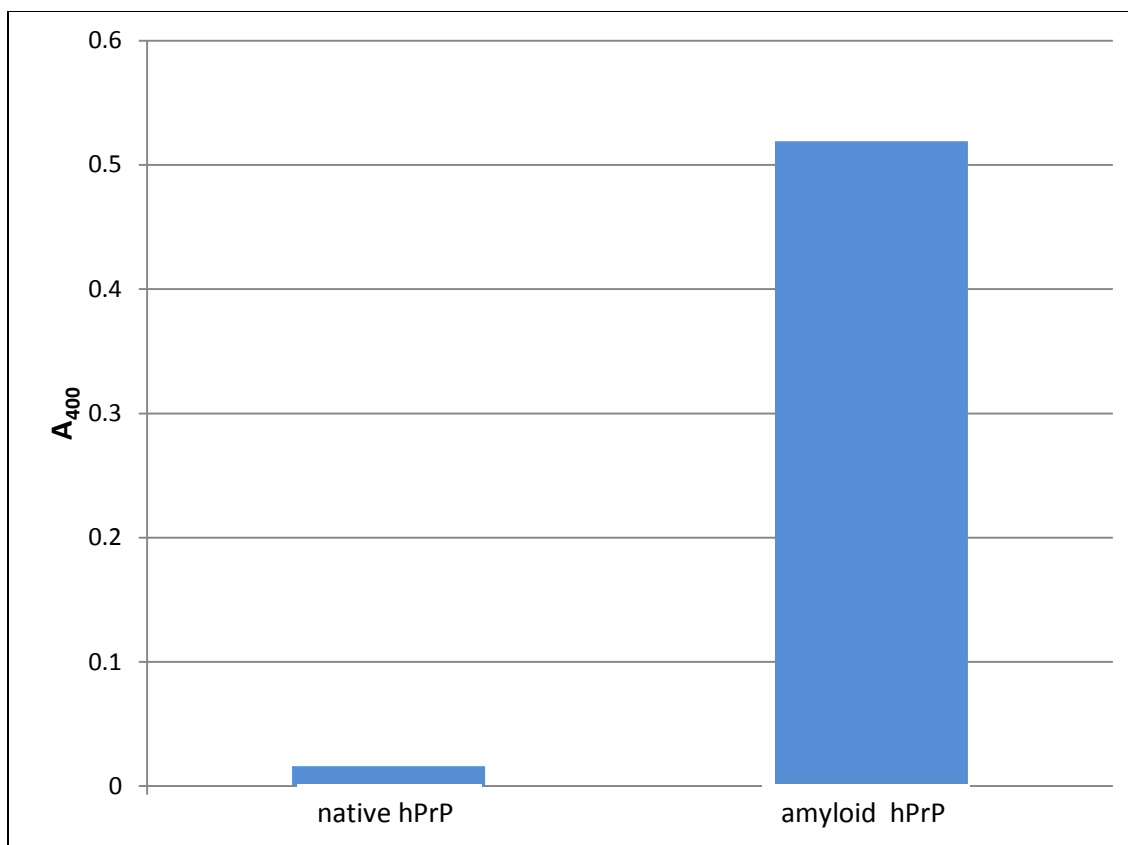


**Figure 2.9. Turbidity of natively folded recombinant hPrP relative to amyloid hPrP.** The absorbance of each sample was measured at 400 nm ( $A_{400}$ ). The left column represents the absorbance of a sample containing 25  $\mu$ M recombinant hPrP, 1X PBS, 0.1% SDS, 0.1% TritonX-100. The right column is the absorbance of a sample containing 0.5 mg/mL of amyloid hPrP in 1X PBS, 0.1% SDS, 0.1% TritonX-100.

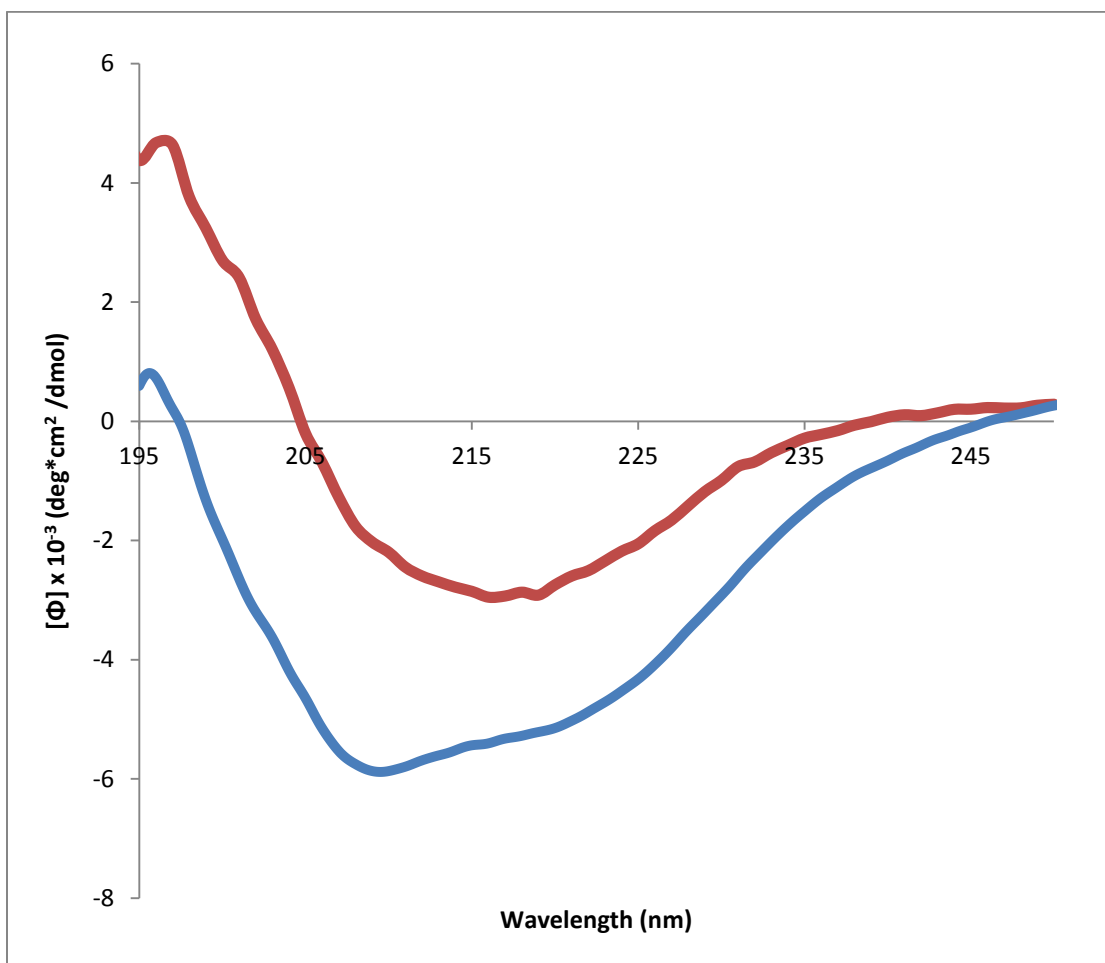


**Figure 2.10. Far UV-CD spectra of natively folded and amyloid hPrP.** The blue line represents native recombinant hPrP (0.5mg/mL) in 20mM Na<sub>2</sub>HPO<sub>4</sub> at pH 7.0. The red line represents amyloid hPrP (estimated to be 0.5mg/mL) in 1X PBS.

rate of 5 liters per minute. All spectra were measured at 20°C in a 1 mm quartz cuvette and used a 300 µL sample of 0.5 mg/mL hPrP in 20 mM sodium phosphate at pH 7.0. A scan rate of 50 nm per minute in 1 nm steps was used and 50 scans were averaged for each measured spectrum. The raw output data from the spectropolarimeter were given in ellipticity ( $\theta$ ) and represent the rotation of plane polarized light in millidegrees. The ellipticity was then normalized to mean molar ellipticity per residue in degrees ( $\theta_{mrd}$ ) using the equation:

$$\theta_{mrd} = \theta \cdot \frac{M}{10 \cdot c \cdot l \cdot n} \left[ \frac{\text{deg} \cdot \text{cm}^2}{\text{dmol} \cdot \text{residue}} \right], \quad (2.2)$$

where  $M$  was the molecular weight of hPrP (22.86 kDa),  $c$  its molar concentration,  $l$  the path length, and  $n$  the number of residues.

#### 2.4.5 Estimating the amount hPrP amyloid in a sample by the Bradford Assay

A Bradford assay was used to estimate the amount of amyloid hPrP in a sample. In brief, a protein standard was made using a 2 mg/mL stock of bovine  $\gamma$ -globulin (BGG) purchased from G-Biosciences (St. Louis, MO). The protein standard was diluted to 1, 0.5, 0.2, 0.1, 0.05, and 0.02 mg/mL concentrations and mixed with Bradford reagent (described below) at a ratio of 10 µL of standard to 100 µL of Bradford reagent. The standard solutions were incubated for 15 minutes at room temperature and then used to generate a standard curve by measuring sample absorbance at 595 nm, relative to a blank consisting of only the Bradford reagent. All absorbance measurements used a 1 cm quartz micro-cuvette. The amyloid in a sample of hPrP was first isolated by centrifugation at 16,000xg for 1 hour. The supernatant was decanted and the fibril pellet resuspended in

100  $\mu$ L of 1X PBS using gentle sonication. 10  $\mu$ L of the fibril solution was then mixed with 100  $\mu$ L of Bradford reagent and incubated for 15 minutes at room temperature. The absorbance of this sample was measured at 595 nm relative to a blank consisting of only the Bradford reagent. By direct comparison to the standard curve, the concentration of protein in the resuspended fibril solution was estimated and used to report on the amount of amyloid in the original hPrP sample.

The Bradford reagent was made by dissolving 50 mg of coomassie blue G-250 in 50 mL of methanol, followed by the addition of 100 mL of 85% phosphoric acid. The coomassie + methanol + phosphoric acid solution was then mixed with 500 mL of dH<sub>2</sub>O and filtered using standard 494-grade paper purchased from VWR Scientific (Radnor, PA). Lastly, water was added to 1 L and the solution stored at 4°C in a foil-wrapped bottle.

## ***2.5 Methods to Promote the Structural Conversion of Natively-Folded Recombinant hPrP to Amyloid Oligomers***

### ***2.5.1 De novo amyloidosis induced by peptide:hPrP binding interactions***

The ability of small peptides to interact with purified and natively folded hPrP and induce the formation of hPrP amyloid was tested by mixing peptide and hPrP at concentrations of 1 mM and 4.3  $\mu$ M, respectively, in 100  $\mu$ L solutions of 1X PBS, 0.1% SDS, and 0.1% TritonX-100 at pH 7.0. The samples were incubated for up to 72 hours at 37°C in an Eppendorf Thermomixer R (Hauppauge, NY) with 1-minute pulses of agitation separated by 1-minute periods of rest. Agitation consisted of rapid shaking of the sample at 1500 RPM. The presence of amyloid in any sample was then tested using

the amyloid detection methods outlined in sections 2.4.1 through 2.4.4. Following commercial synthesis, all peptides stocks were solubilized in DNA grade sterile water (protease-free) to concentrations of 10 mM and stored at -20°C in sterile cryovial tubes.

### 2.5.2 *Amyloidosis induced by providing amyloid particles as nucleating seeds*

A key property of prion amyloid is its ability to act as nucleating seeds to propagate the amyloid state in fresh PrP<sup>C</sup>.<sup>2</sup> To test for this property in the peptide-induced amyloid particles made by the method outlined in section 2.5.1, the following protocol was used. First, peptide + hPrP samples were tested for the presence of amyloid using amyloid detection methods (see sections 2.4.1 through 2.4.4). Samples shown to have amyloid were centrifuged at 16,000xg, room temperature, using a Beckman Coulter Benchtop Microfuge (Fullerton, California). Centrifugation had the effect of pelleting the insoluble fibrils and separating them from the rest of the sample. After centrifugation, the supernatant was decanted and the fibrils were suspended in 100 µL of molecular biology grade sterile 1X PBS. Next, the suspended fibrils were gently sonicated using a Bronson Sonifier S-450A (Danbury, CT) to create smaller-sized amyloid oligomers. This was done for two reasons: 1) to increase the solubility of the amyloid particles in 1X PBS, and 2) to decrease the size of the larger fibrils that were so long they resisted transfer by micropipette tips. During sonication, the sample was kept on ice to prevent heating. The sonication procedure consisted of three 1-minute pulses separated by 1-minute rest periods, with the sonifier set to a duty cycle of 20% and an output control of 1. Then, 10 µL of the sonicated amyloid solution was added to a solution of freshly purified and natively folded hPrP to make a 100 µL sample of 4.3 µM hPrP, 1X PBS, 0.1% SDS, 0.1% TritonX-100. The sample of fresh hPrP + amyloid seed was then incubated for up

to 72 hours at 37°C in an Eppendorf Thermomixer R (Hauppauge, NY) with 1-minute pulses of agitation separated by 1-minute periods of rest. Agitation consisted of rapid shaking of the sample at 1500 RPM. The amount of amyloid in any sample was estimated using the amyloid detection methods discussed above.

## CHAPTER III

### AMYLOID MISFOLDING OF NATIVE RECOMBINANT HUMAN PRION PROTEIN INDUCED BY PEPTIDE INTERACTIONS

#### 3.1 *Introduction*

The structural conversion of cellular protein from its normal physiological state to amyloid oligomers is associated with several terminal human disorders, including Alzheimer's, Parkinson's, and the prion diseases.<sup>12</sup> Detailed characterization of protein amyloidosis is clearly needed to understand this class of diseases, however, experimental data on amyloid structural transitions are limited. To better understand the molecular interactions that facilitate amyloidosis, peptide ligands were designed to bind to the human prion protein (hPrP) and promote its self-assembly into amyloid oligomers. The prion protein was chosen for this study because an unknown protein cofactor has been hypothesized to interact with hPrP, suggesting that hPrP:ligand interactions may indeed be important in the molecular pathology of prion diseases.<sup>28</sup> Preliminary results using tissue-derived prion protein show that small peptides containing the sequence KFAKF may promote amyloidosis, which was presented in Chapter I, section 1.3, of this thesis.

To exercise tighter control over this experimental strategy for studying binding interactions that promote amyloid self-assembly, a recombinant system for synthesizing natively-folded hPrP and observing prion misfolding was developed. This system will allow us to investigate residue-specific interactions, both in terms of hPrP and the peptide cofactor, that are salient to prion amyloidosis, which is the basis of future studies. In the current study, bacterially expressed recombinant hPrP was purified and shown to fold into its native physiological state that is predominantly  $\alpha$  helical. It is also shown that native hPrP can be induced into amyloid oligomers under normal solution conditions (1X PBS, 37°C), through interactions with a peptide cofactor. The *de novo* conversion of natively-folded recombinant hPrP to amyloid was detected using a battery of amyloid-detection techniques based on circular dichroism, resistance to protease digestion, light scattering, and a fluorimetric thioflavin T binding assay. Lastly, it is shown that amyloid particles formed from the hPrP:peptide reactions can seed the self-assembly of fresh hPrP to amyloid in the absence of peptide cofactors.

## **3.2 Results and Discussion**

### **3.2.1 Purification and native folding of recombinant hPrP**

Recombinant human prion protein (hPrP) was expressed in *E. coli* cells and purified from cell lysate using Ni<sup>2+</sup> affinity chromatography, as detailed in Chapter 2, section 2.2, of this thesis. The purity of hPrP obtained in this manner was judged to be greater than 99% by silver staining of samples electrophoresed using SDS-PAGE techniques (see Figure 2.4). The identity of the purified protein was verified as hPrP by western blot analysis using the monoclonal antibody 3F4 (see Figure 2.5).

Overnight dialysis was used to transfer hPrP to a phosphate buffered solution (20 mM Na<sub>2</sub>HPO<sub>4</sub>, pH 7.0) for CD spectral measurements and to check for correct folding. The CD spectrum of hPrP was measured at 20°C and showed that this protein was natively folded by comparison to the CD spectrum of native prion protein published by other research groups.<sup>12</sup> The CD spectrum of native hPrP displays the characteristic minima at 208 nm and 222 nm that are hallmark signatures of a protein that is folded predominantly into  $\alpha$  helices<sup>49</sup>, and is shown in Figure 3.1. These data demonstrate that hPrP used in our studies was initially folded into its correct native state.

### 3.2.2 *Peptide-induced amyloidosis of recombinant hPrP*

The ability of small peptides containing the sequence KFAKF to promote amyloidosis of natively folded hPrP was tested by mixing protein and peptide to final concentrations of 4.3  $\mu$ M hPrP and 1 mM peptide in 1X PBS, 0.1% SDS, 0.1% TritonX-100. These solution conditions were chosen to mimic the solution conditions used in PMCA assays by Soto's group.<sup>30</sup> The peptides tested were synthesized commercially by GenScript (Piscataway, NJ) and Peptide 2.0 (Chantilly, VA) and are listed in Table 3.1. Each hPrP + peptide sample was incubated at 37°C with periodic and gentle sonication, as described in the Methods (section 2.5.1).

The structural conversion of natively folded recombinant hPrP to amyloid in each sample was tested using multiple amyloid detection techniques. Shown in Figure 3.2 are the results of incubating hPrP with the cyclic peptide cyclo-CGGKFAKFGGC (referred to as peptide-3) for up to 72 hours, as monitored by the fluorescence of Thioflavin T (ThT). ThT fluorescence near 480 nm increases dramatically when amyloid oligomers are

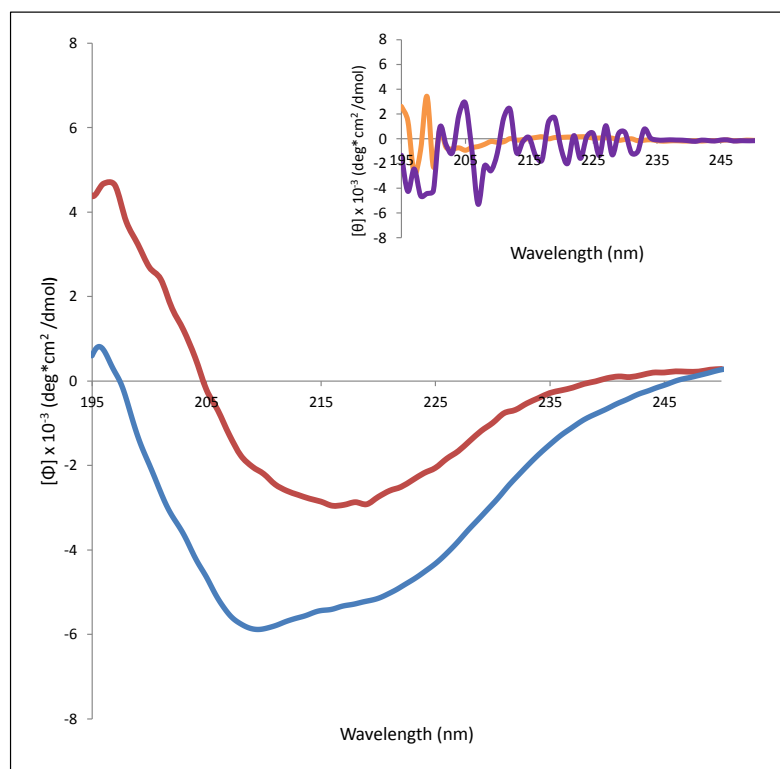


**Figure 3.1. Far UV-CD spectra of natively folded and peptide-3-induced hPrP amyloid.** The blue line represents native recombinant hPrP (0.5mg/mL) in 20mM  $\text{Na}_2\text{HPO}_4$  at pH 7.0. The red line represents peptide-3-induced hPrP amyloid (estimated to be 0.5mg/mL) in a solution that is approximately 1X PBS. The purple line in the inset shows the CD spectrum of 1X PBS, 0.1% SDS, 0.1% TritonX-100. The noise in the CD signal from 200 – 235 nm is due to the optical activity of TritonX-100. The orange line shows the same sample after 4 cycles of concentrating then diluting the sample with 1X PBS using a centrifugal concentrating filter. Note that the signal noise from 200 – 235 nm has been significantly weakened.

**Table 3.1.** Synthetic peptides tested for the ability to promote amyloidosis of recombinant hPrP.

<b>Peptide Name</b>	<b>Peptide Sequence</b>
Peptide-1	KFAKF
Peptide-2	cyclo-CGKFAKFGC
Peptide-3	cyclo-CGGKFAKFGGC

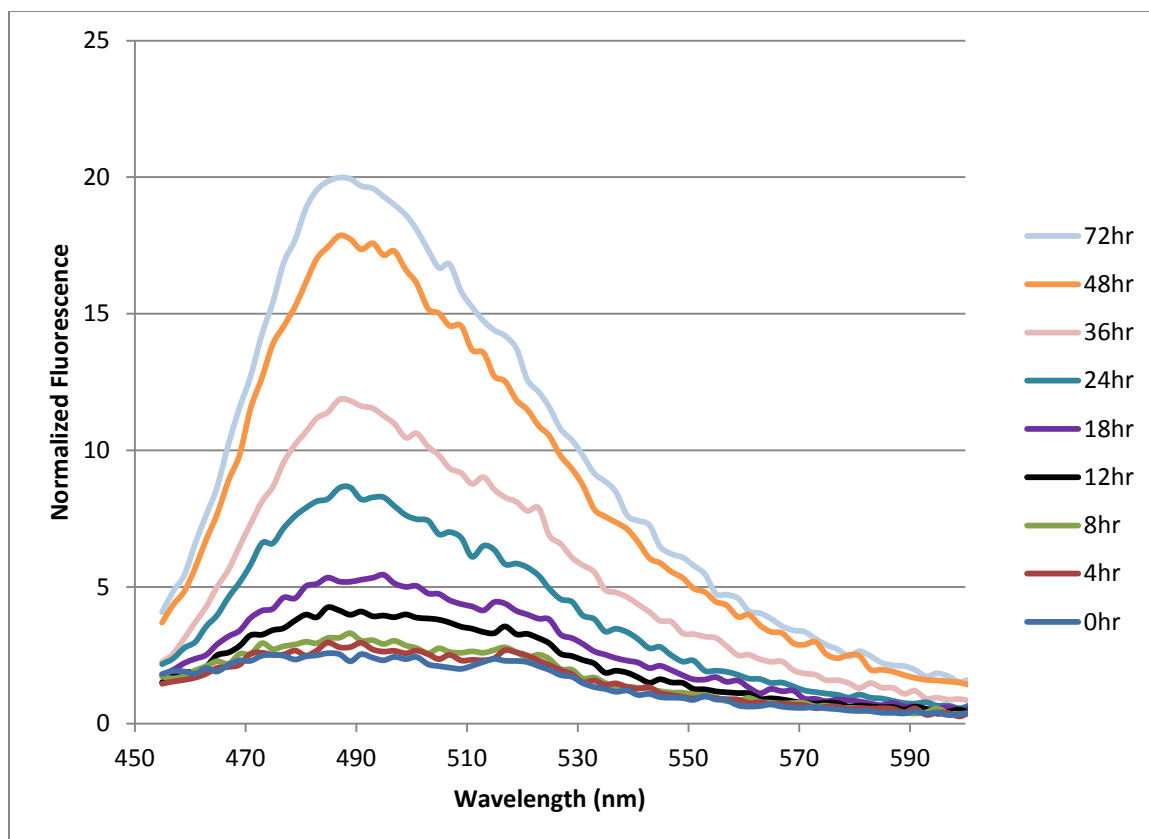


**Figure 3.2. Fluorescence spectra of samples containing hPrP + cyclo-CGGKFAKFGGC, incubated from 0 to 72 hours.** Each sample contained 4.3  $\mu\text{M}$  hPrP, 1 mM cyclo-CGGKFAKFGGC, 1X PBS, 0.1% SDS, 0.1% TritonX-100 and was incubated at 37°C as indicated. 15  $\mu\text{L}$  of each sample was individually mixed with 985  $\mu\text{L}$  of 10  $\mu\text{M}$  ThT, 50 mM glycine, pH 8.5 and its emission spectrum was measured using an excitation wavelength of 442 nm.

present and the sample is excited at 442 nm.<sup>47</sup> As can be seen in the figure, at the initial time point (0 hr), there was minimal sample fluorescence suggesting no amyloid was present. Over the course of 72 hours, the sample fluorescence increased substantially, suggesting that amyloid particles formed over time in the sample. Samples containing hPrP only or peptide-3 only showed no fluorescence increase, relative to the initial sample fluorescence, for incubation times up to 48 hours (Figure 3.3). Samples containing hPrP + cyclo-CGKFAKFGC (peptide-2) or hPrP + KFAKF (peptide-1) also gave no detectable fluorimetric signal for amyloid in samples incubated as long as 72 hours (Figure 3.4). These experiments were repeated an additional 3 times, for a total of 4 trials, and displayed good reproducibility. The cumulative results of peptide-3-induced amyloidosis of hPrP as monitored by ThT fluorescence is given in Figure 3.5 for the 4 trials. These data suggest that peptide-3 interacts with recombinant hPrP to promote amyloid misfolding, while the other two synthetic peptides that were tested do not.

The ability of the three synthetic peptides to misfold hPrP into amyloid was also monitored by an enzymatic digestion assay using Proteinase K (PK). Natively folded hPrP is readily hydrolyzed by PK digestion. In contrast, amyloid prions are partially resistant to PK digestion and produce a 16 kDa fragment that can be observed by western blot analysis.<sup>32</sup> Only samples that contained both hPrP and peptide-3 and that were incubated for at least 8 hours resulted in particles that resisted PK digestion and produced a 16 kDa fragment - consistent with hPrP amyloidosis. These results are shown in Figure 3.6. Of note, samples incubated for less than 8 hours were fully digested by PK, suggesting that peptide-3 does not inhibit PK activity. Samples of hPrP only were also

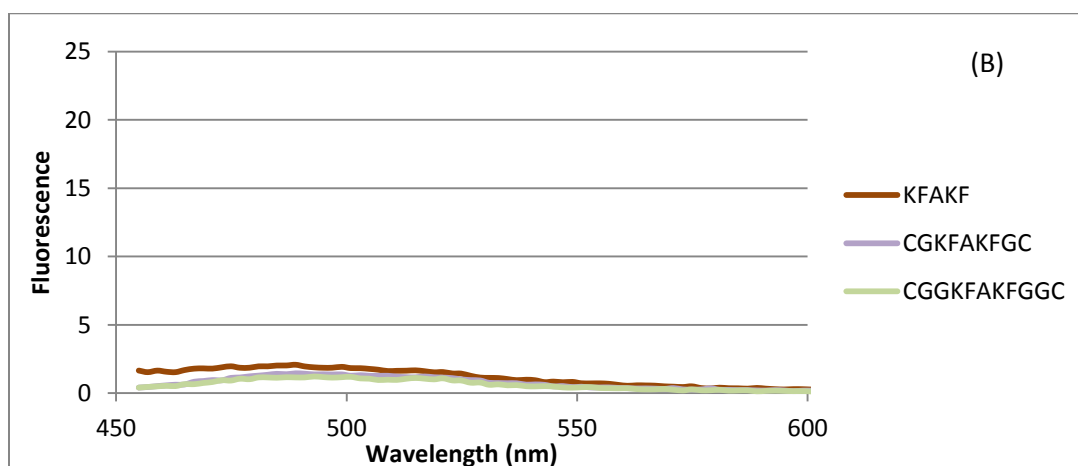
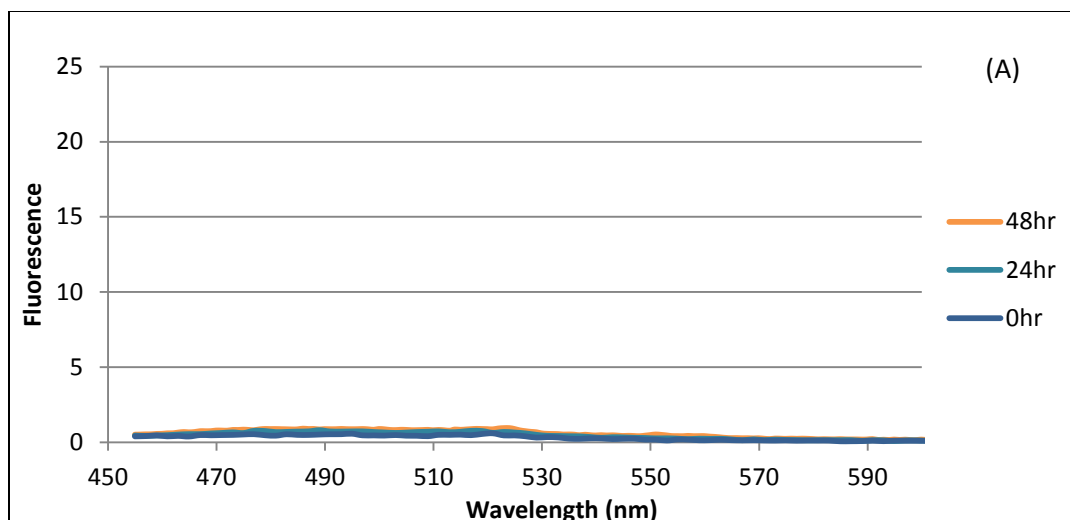


**Figure 3.3. ThT fluorescence when mixed with hPrP only or the synthetic peptides only.** (A) Fluorescence spectra for samples containing 4.3  $\mu\text{M}$  hPrP, 1X PBS, 0.1% SDS, 0.1% TritonX-100 and incubated at 37°C as indicated. 15  $\mu\text{L}$  of each sample was individually mixed with 985  $\mu\text{L}$  of 10  $\mu\text{M}$  ThT, 50 mM glycine, pH 8.5 and its emission spectrum was measured using an excitation wavelength of 442 nm. (B) Fluorescence spectra for samples containing 1X PBS, 0.1% SDS, 0.1% TritonX-100 + 1 mM KFAKF (maroon) or + 1 mM cyclo-CGKFAKFGC (violet) or + 1 mM cyclo-CGGKFAKFGGC (light green) and incubated at 37°C for 48 hours. 15  $\mu\text{L}$  of each sample was individually mixed with 985  $\mu\text{L}$  of 10  $\mu\text{M}$  ThT, 50 mM glycine, pH 8.5 and its emission spectrum was measured using an excitation wavelength of 442 nm.

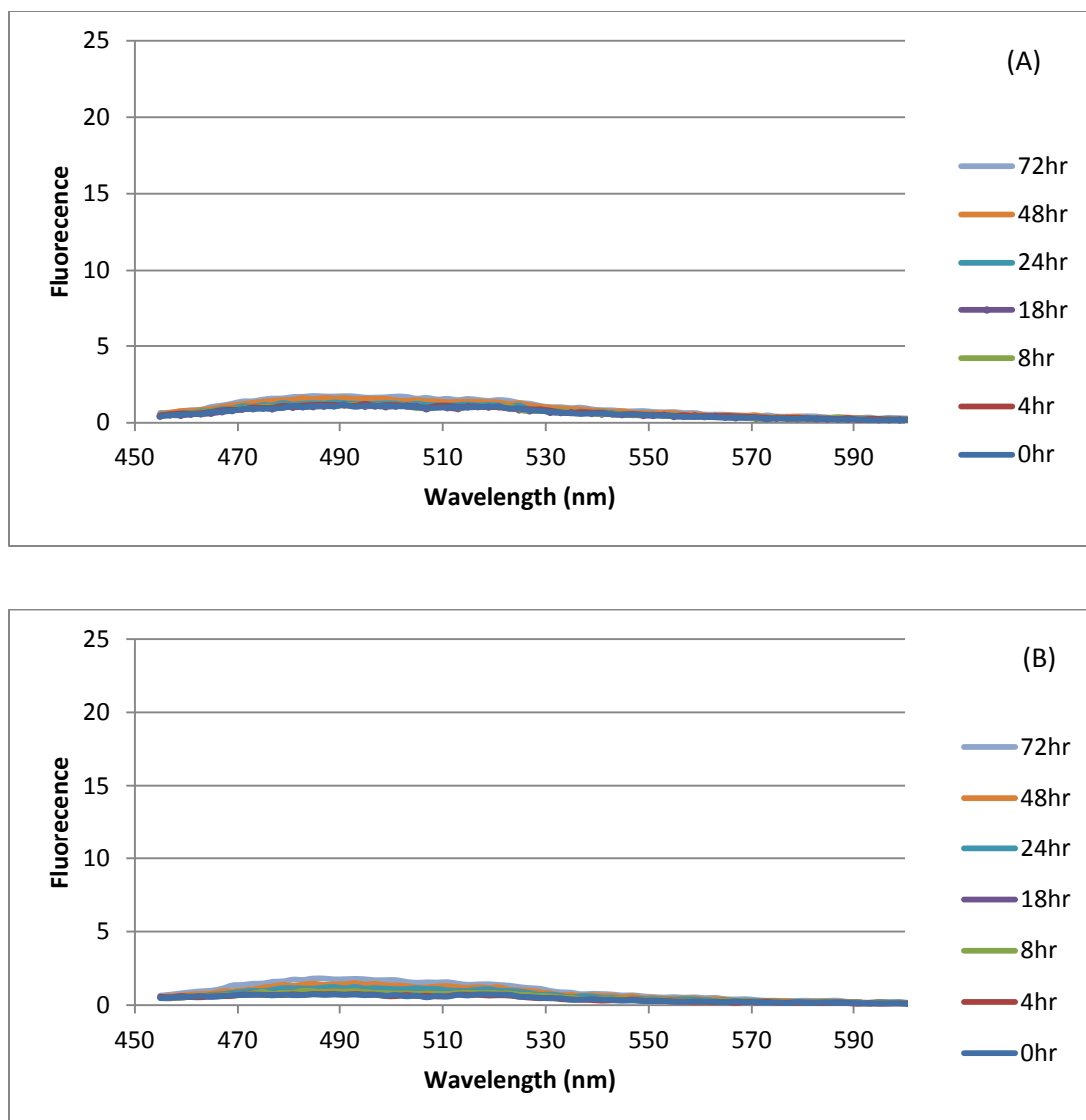


**Figure 3.4. Fluorescence spectra of samples containing hPrP + KFAKF or hPrP + cyclo-CGKFAKFGC, and incubated from 0 to 72 hours.** Each sample contained 4.3  $\mu\text{M}$  hPrP, 1X PBS, 0.1% SDS, 0.1% TritonX-100 and was incubated at 37°C as indicated. Samples in (A) included 1 mM KFAKF. Samples in (B) included 1 mM cyclo-CGKFAKFGC. 15  $\mu\text{L}$  of each sample was individually mixed with 985  $\mu\text{L}$  of 10  $\mu\text{M}$  ThT, 50 mM glycine, pH 8.5 and its emission spectrum was measured using an excitation wavelength of 442 nm.

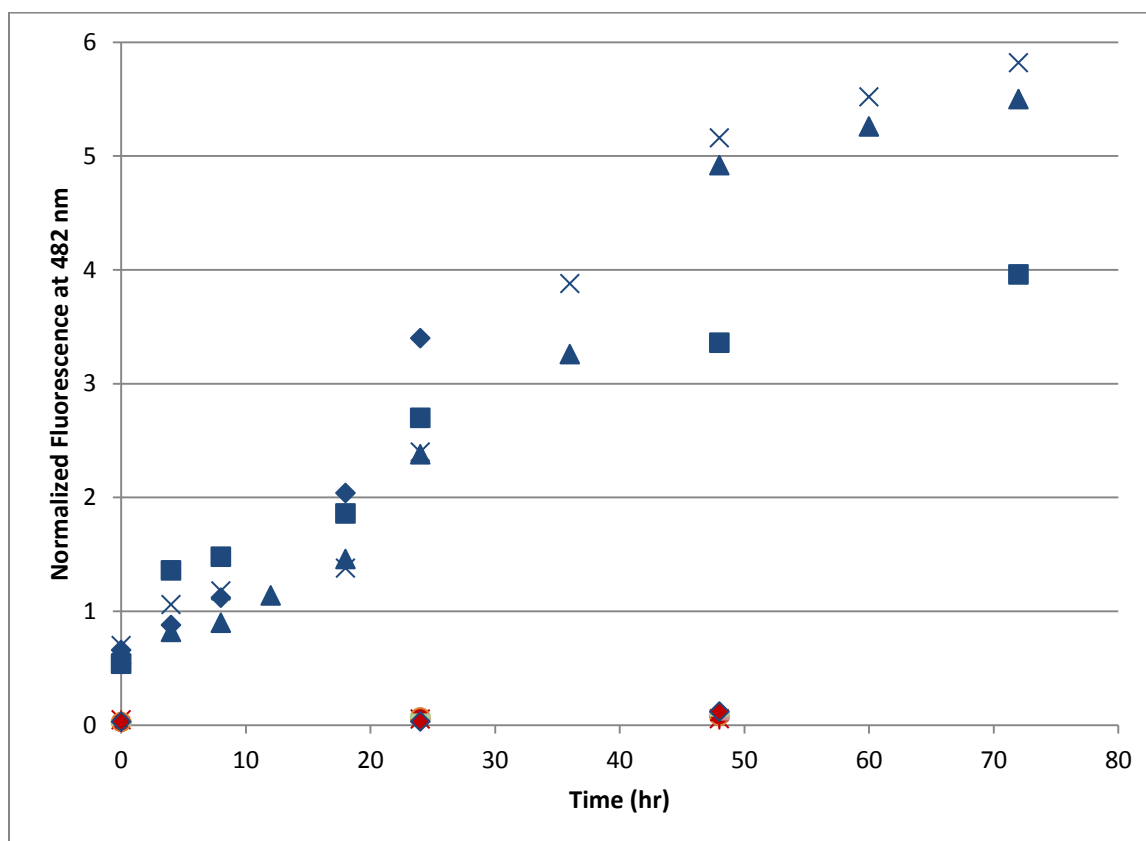


**Figure 3.5. Fluorescence at 482 nm for quadruplicate samples containing hPrP + cyclo-CGGKFAKFGGC.** Each sample contained 1X PBS, 0.1% SDS, 0.1% TritonX-100 and was incubated at 37°C for the time indicated in the figure. 15  $\mu$ L of each sample was individually mixed with 985  $\mu$ L of 10  $\mu$ M ThT, 50 mM glycine, pH 8.5 and its fluorescence emission at 482 nm was measured using an excitation wavelength of 442 nm. Dark blue symbols represent samples that contained 4.3  $\mu$ M hPrP and 1 mM cyclo-CGGKFAKFGGC; the different symbols (squares, triangles, diamonds, and cross marks) represent different trial sets. The symbols in red represent control samples that contained 4.3  $\mu$ M hPrP (diamonds, cross marks, and circles) or 1 mM cyclo-CGGKFAKFGGC (triangles, squares, and stars). To compare sample fluorescence measured from different trials performed on different dates, each data point in this figure was normalized to the measured fluorescence at 430 nm for the ThT solution alone (10  $\mu$ M ThT, 50 mM glycine, pH 8.5), due to an excitation wavelength of 342 nm.

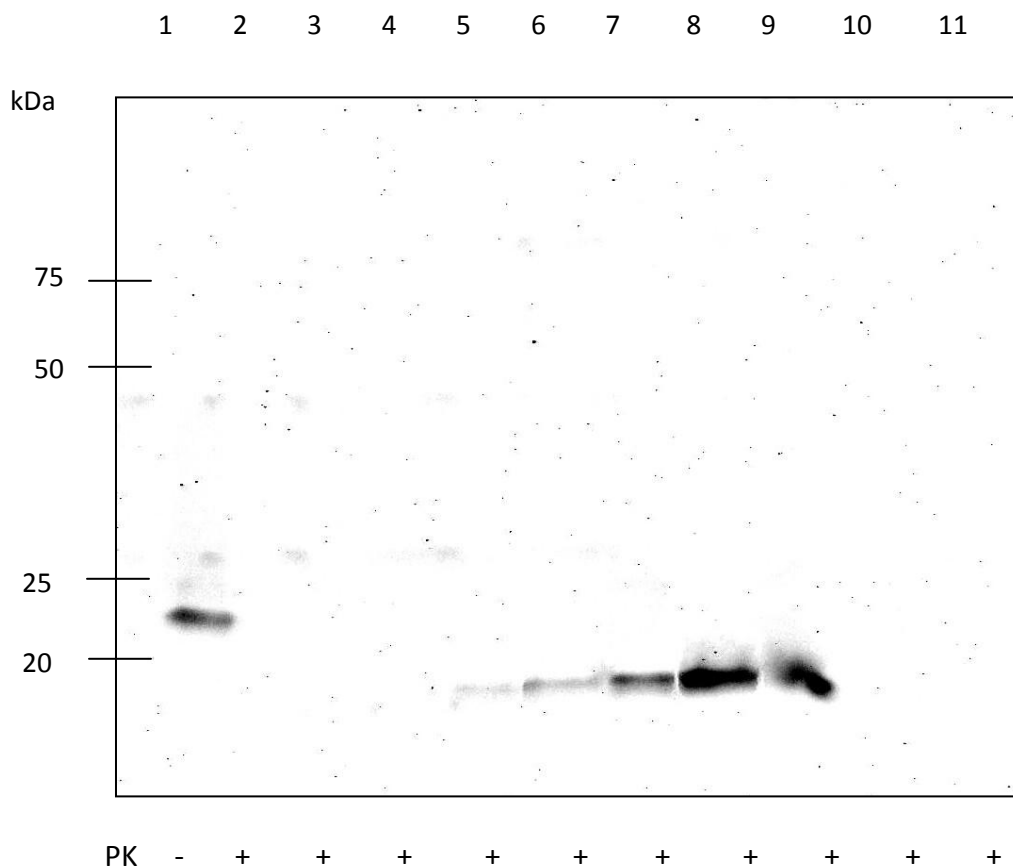


**Figure 3.6. Proteinase K digestion of recombinant hPrP.** Shown is the PK digestion of samples containing 4.3  $\mu$ M hPrP, 1 mM cyclo-CGGKFAKFGGC, 1X PBS, 0.1% SDS, 0.1% TritonX-100 and incubated at 37°C for 0 to 72 hours. Lane 1 is a control, showing an undigested sample without 1 mM cyclo-CGGKFAKFGGC added and at the initial time point (0 hr). Lane 2 is another control, at the 0 hr time point and without 1 mM cyclo-CGGKFAKFGGC added, but digested by PK. Lanes 3 through 9 show PK digested samples incubated for 0, 4, 8, 18, 24, 48, and 72 hours. Lane 10 shows PK digestion of a sample containing 1 mM KFAKF instead of cyclo-CGGKFAKFGGC and incubated for 48 hours. Lane 11 shows PK digestion of a sample containing 1 mM cyclo-CGKFAKFGC instead of cyclo-CGGKFAKFGGC and incubated for 48 hours. After completion of the western blot protocol, the polyacrylamide gel was stained with coomassie to view molecular weight standards that were electrophoresed in an additional lane. The positions of the molecular weight standards are estimated in the gel image based upon their coomassie-stained positions.

fully digested by PK. This is shown in lane 2 of the Figure 3.6 gel image, but was also true for samples containing only hPrP and incubated for up to 72 hours (data not shown). Samples containing hPrP + peptide-2 or hPrP + peptide-1 and incubated for up to 72 hours were also fully digested by PK, suggesting no amyloid conversion. Western blot results for samples containing hPrP + peptide-2 and hPrP + peptide-1 incubated for 48 hours are shown in lanes 10 and 11, respectively, of the Figure 3.6 gel image.

Samples of hPrP + peptide-3 were also tested for amyloid by light scattering and CD spectroscopy. Solutions containing amyloid fibrils are visibly turbid and scatter light at 400 nm.<sup>48</sup> As can be seen in Figure 3.7, samples of hPrP + peptide-3 scatter light at progressively greater amounts for samples that were incubated from 0 to 72 hours, which is consistent with a progressive conversion of natively folded hPrP to amyloid fibrils. To measure the CD spectrum of amyloid misfolded hPrP required additional sample preparation steps, which were required to remove TritonX-100 from the sample. TritonX-100 is optically active and obscures CD measurements. Initially, dialysis-based techniques were tried but proved ineffective. A second strategy that used membrane filtration was successful at removing TritonX-100. This was accomplished by repeated cycles of concentrating the sample using Centriprep centrifugal filters (Millipore, Carrigtwohill, Ireland) that bind TritonX-100 followed by dilution. Four concentration-dilution cycles removed TritonX-100 from the sample to a level that allowed CD measurements (see inset of Figure 3.1). Shown in Figure 3.1 is the CD spectrum of amyloid misfolded hPrP as induced by peptide-3. This CD spectrum shows a negative minimum near 218 nm and a positive maximum at 196 nm, which are associated with  $\beta$  sheet structures<sup>12</sup> and is distinctly different from the CD spectrum of native hPrP.

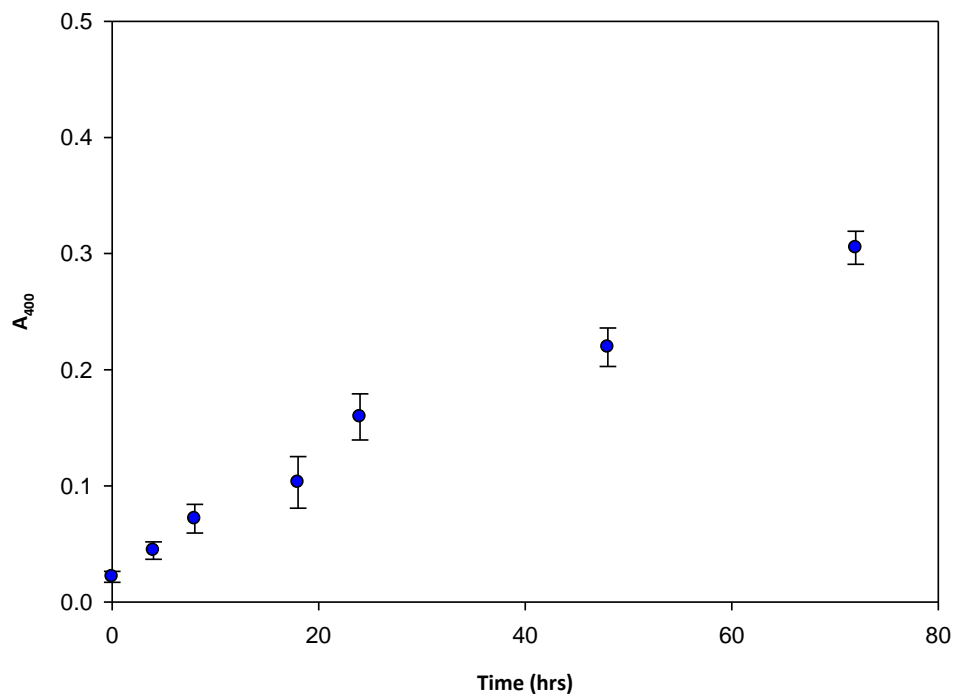


**Figure 3.7. Turbidity of samples containing hPrP + cyclo-CGGKFAKFGGC, incubated from 0 to 72 hours.** Each sample contained 4.3  $\mu$ M hPrP, 1 mM cyclo-CGGKFAKFGGC, 1X PBS, 0.1% SDS, 0.1% TritonX-100 and was incubated at 37°C as indicated. The absorbance of each sample was measured at 400 nm ( $A_{400}$ ). Each data point in the figure is an average from the experiment being performed in triplicate. The error bars represent the standard deviation in each averaged value.

### 3.2.3 *Non-amyloid aggregation of recombinant hPrP*

Recombinant hPrP has poor solubility and aggregates over time under normal solution conditions. Samples containing 25  $\mu\text{M}$  hPrP, 5 mM Tris-HCl, pH 8.5 and stored at 4°C will form visible precipitates of hPrP over 48 hours. This is shown in Figure 3.8. These hPrP aggregates, however, do not appear to have amyloid character, as indicated by the data presented in Figure 3.9. In panel A, PK is observed to fully digest hPrP aggregates, suggesting that a protease resistant core is not formed and that the aggregates are structurally distinct from amyloid. Similarly, ThT fluorescence assays also indicate that the aggregates are not amyloid (panel B).

### 3.2.4 *hPrP amyloidosis through amyloid seeding*

A key trait of prion amyloid is its ability to interact with non-amyloid prion protein to seed additional amyloid conversion.<sup>20</sup> To test for this property, peptide-3-induced hPrP amyloid were isolated by centrifugation and then resuspended in fresh 1X PBS. Small aliquots containing approximately 100 ng of hPrP amyloid were then used to seed amyloidosis of fresh, natively folded hPrP. Using ThT fluorescence as an indicator, Figure 3.10 demonstrates that at the initial time point (0 hr) the sample contained nearly undetectable amounts of amyloid. Incubation of the sample over 72 hours, however, demonstrated a large increase in ThT fluorescence observed at 480 nm, suggesting extensive conversion of native hPrP to amyloid. Figure 3.11 demonstrates that the turbidity of the sample increased concomitant to the increase in ThT fluorescence, and likewise suggested amyloid conversion of native hPrP.

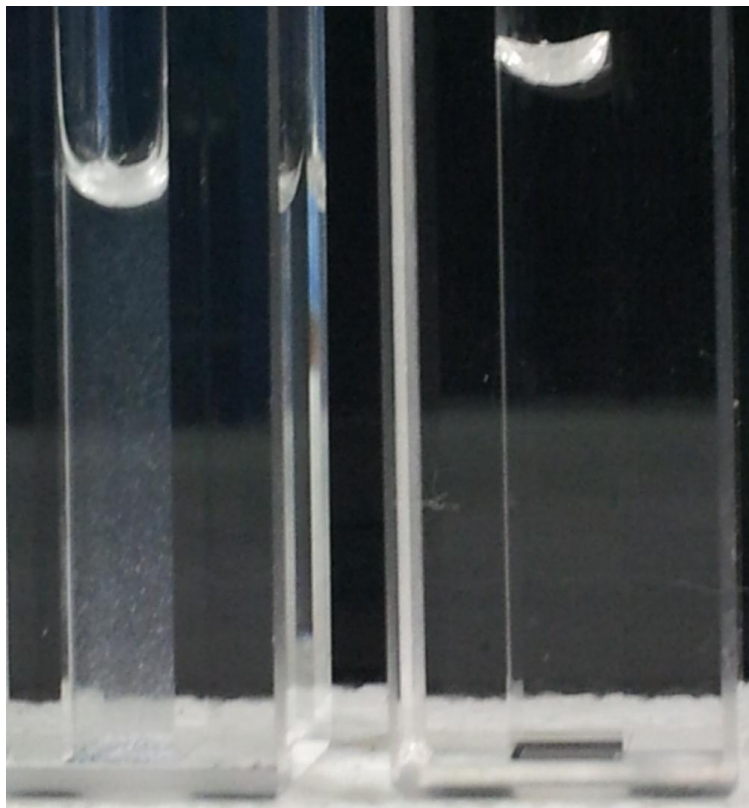


**Figure 3.8. Aggregation of recombinant hPrP.** The cuvette pictured on the left contains 1 mL of 25  $\mu$ M hPrP, 5 mM Tris-HCl, pH 8.5 and was incubated for 48 hours at 4°C. Initially, no precipitates were visible in this sample, but over the 48 hour incubation, aggregates of hPrP appeared. For comparison, the cuvette on the right contains water.

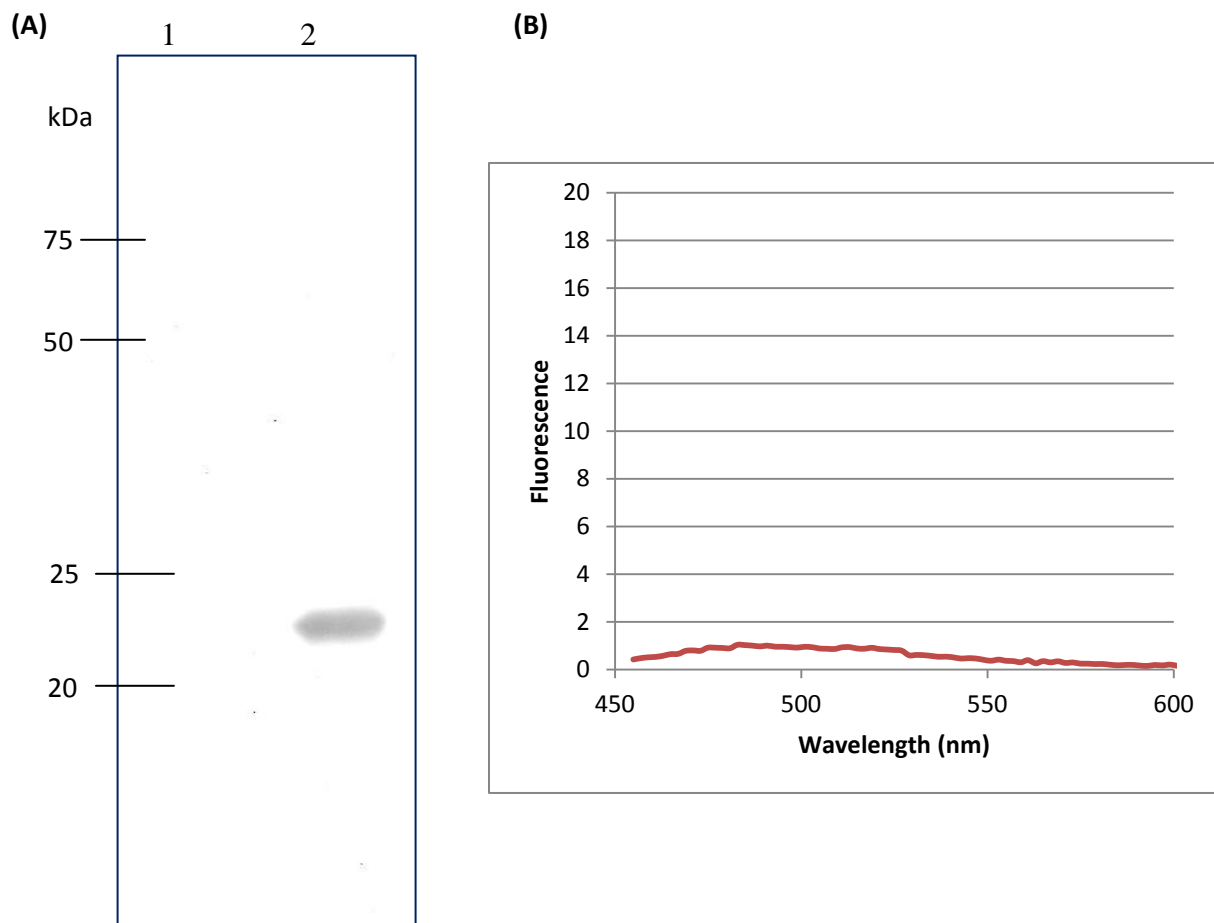


**Figure 3.9. PK digestion and ThT fluorescence of samples containing aggregates of hPrP.** A sample containing 25  $\mu\text{M}$  hPrP, 5 mM Tris-HCl, pH 8.5 was incubated for 48 hours at 4°C to produce hPrP aggregates. An aliquot from this sample was digested by PK, which is shown in panel (A). Lane 1 is PK digestion of the aliquot, whereas lane 2 is without PK digestion. ThT fluorescence was measured by mixing 15  $\mu\text{L}$  of the sample with 985  $\mu\text{L}$  of 10  $\mu\text{M}$  ThT, 50 mM glycine, pH 8.5. This is shown in panel (B) and demonstrates no significant fluorescence from 460 nm – 600 nm. The emission spectrum was measured using an excitation wavelength of 442 nm.

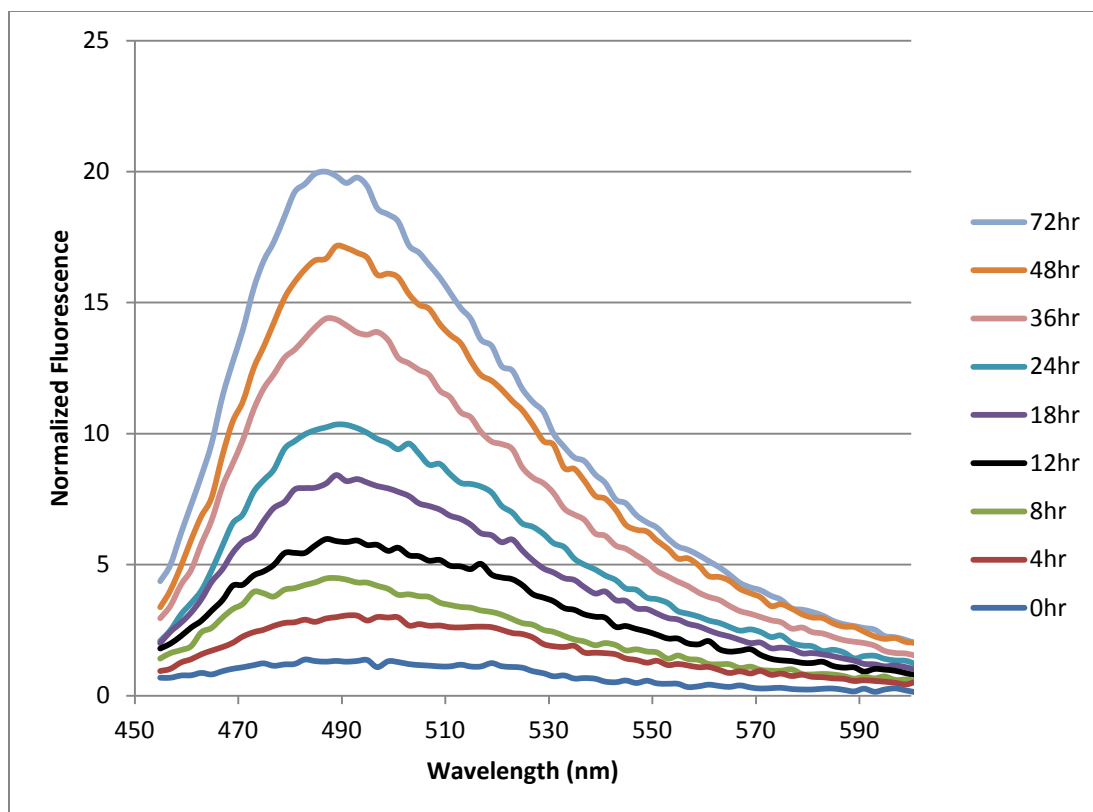


**Figure 3.10. Fluorescence spectra of samples containing hPrP + ~ 100 ng hPrP amyloid, incubated from 0 to 72 hours.** Each sample consisted of 100  $\mu\text{L}$  of 4.3  $\mu\text{M}$  hPrP, 1X PBS, 0.1% SDS, 0.1% TritonX-100 mixed with ~ 100 ng peptide-3-induced hPrP amyloid and was incubated at 37°C as indicated. 15  $\mu\text{L}$  of each sample was individually mixed with 985  $\mu\text{L}$  of 10  $\mu\text{M}$  ThT, 50 mM glycine, pH 8.5 and its emission spectrum was measured using an excitation wavelength of 442 nm.

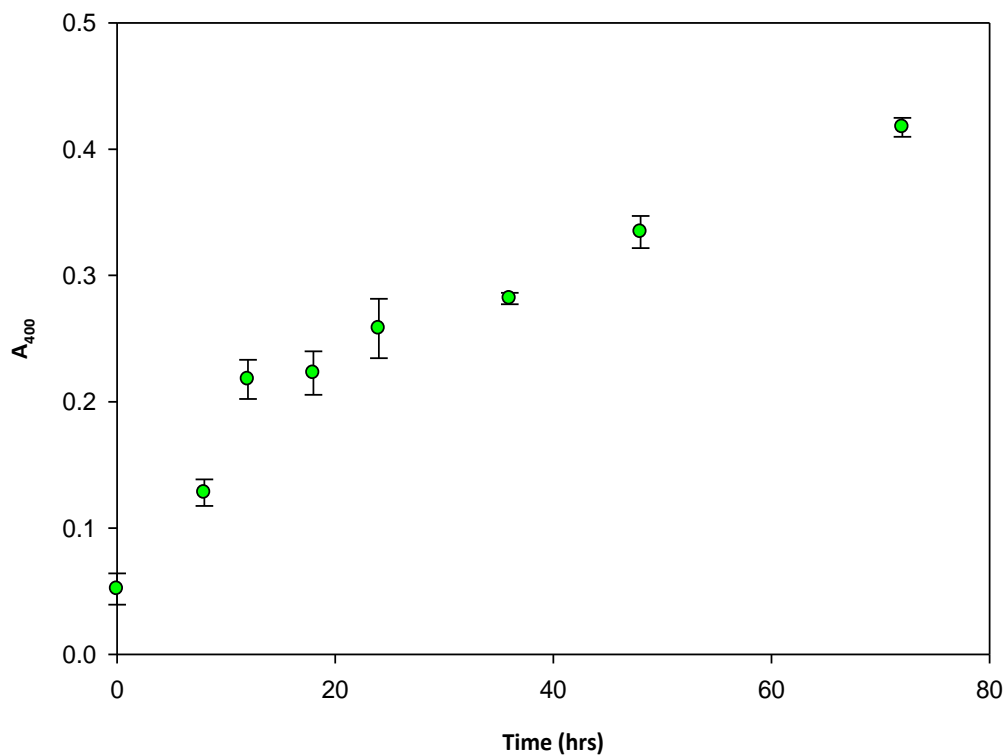


**Figure 3.11. Turbidity of samples containing hPrP + ~ 100 ng hPrP amyloid, incubated from 0 to 72 hours.** Each sample consisted of 100  $\mu$ L of 4.3  $\mu$ M hPrP, 1X PBS, 0.1% SDS, 0.1% TritonX-100 mixed with ~ 100 ng peptide-3-induced hPrP amyloid and was incubated at 37°C as indicated. The absorbance of each sample was measured at 400 nm ( $A_{400}$ ). Each data point in the figure is an average from the experiment being performed in triplicate. The error bars represent the standard deviation in each averaged value.

To test if the observed hPrP amyloidosis resulted from dilute amounts of peptide-3 present in the seeding aliquot, a fresh sample of natively folded hPrP was incubated with 0.1 mM peptide-3 for 72 hours. This is the maximum peptide-3 concentration that could be present in the seeded reactions of Figures 3.10 and 3.11, based on the protocol used (see Chapter 2, section 2.5.2). Figure 3.12 demonstrates that no significant amyloid conversion was observed in samples of hPrP + 0.1 mM peptide-3, even after the sample was incubated for 72 hours. These results suggest that hPrP amyloidosis induced by the amyloid seeds were not the result of dilute amounts of peptide-3.

### 3.3 Conclusions

The molecular pathology of prion amyloidosis is currently the subject of extensive study and debate.<sup>23</sup> Based on a controversial hypothesis that a host-provided cofactor dubbed "protein X" is necessary for PrP<sup>Sc</sup> to self-replicate *in vivo*<sup>17</sup>, peptide ligands using the sequence motif of KFAKF were designed to mimic protein X interactions with the prion protein and promote hPrP amyloidosis *in vitro*. The peptides synthesized and tested for amyloidogenic properties were: 1) a short linear peptide with the sequence KFAKF, 2) a cyclic version of the linear peptide (cyclo-CGKFAKFGC), and 3) a slightly larger cyclic version (cyclo-CGGKFAKFGGC). Of these, only the larger cyclic peptide (cyclo-CGGKFAKFGGC) was observed to induce hPrP amyloidosis, as demonstrated using four different experimental assays (ThT fluorescence, protease resistance, sample turbidity, and CD spectroscopy). The relationship of cyclo-CGGKFAKFGGC to any physiological cofactors found in humans has not been investigated and will be the basis of future studies. It has been recognized that

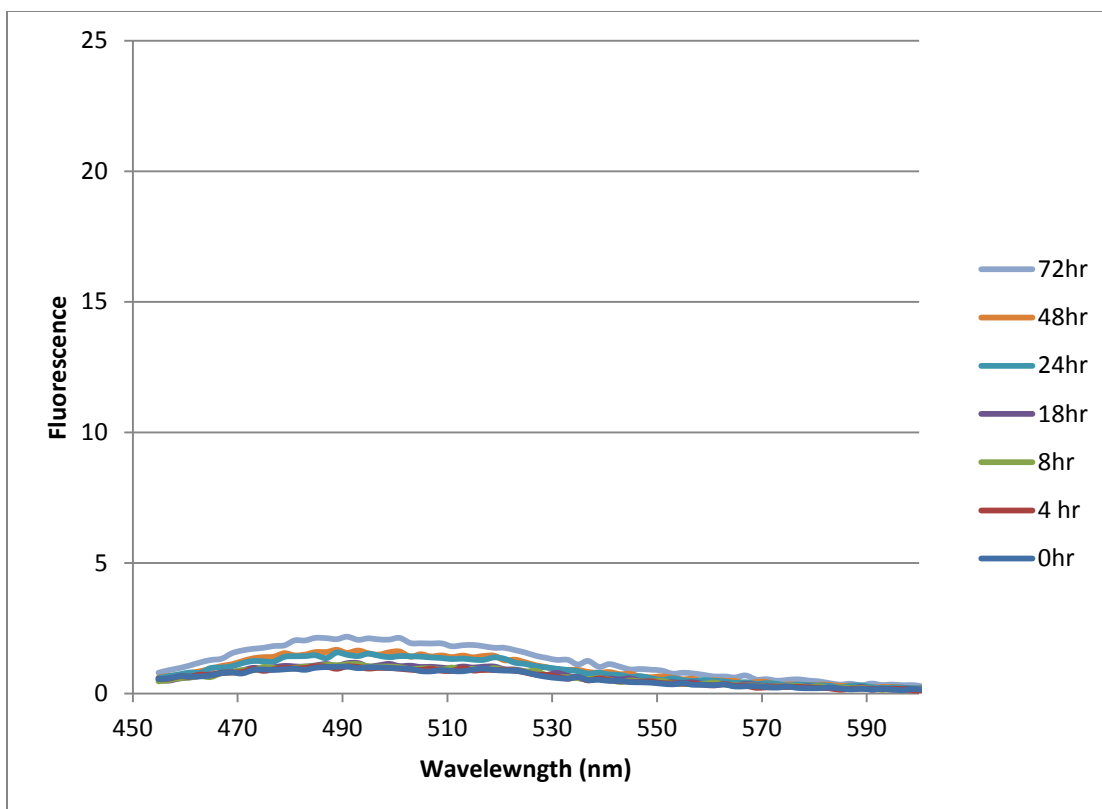


**Figure 3.12. Fluorescence spectra of samples containing hPrP + 0.1 mM cyclo-CGGKFAKFGGC, incubated from 0 to 72 hours.** Each sample contained 4.3  $\mu\text{M}$  hPrP, 0.1 mM cyclo-CGGKFAKFGGC, 1X PBS, 0.1% SDS, 0.1% TritonX-100 and was incubated at 37°C as indicated. 15  $\mu\text{L}$  of each sample was individually mixed with 985  $\mu\text{L}$  of 10  $\mu\text{M}$  ThT, 50 mM glycine, pH 8.5 and its emission spectrum was measured using an excitation wavelength of 442 nm.

KFAKF sequence is homologous to a class of neuropeptides common to mammals, which are referred to as RF-amide peptides. In chapter 4, we will investigate peptide-induced hPrP amyloidosis using synthetic peptides with sequences based on an RF-amide peptide sequence.

## CHAPTER IV

### PEPTIDE HOMOLOGS TO THE RF-AMIDE CLASS OF NEUROPEPTIDES INDUCE AMYLOID MISFOLDING OF RECOMBINANT HUMAN PRION PROTEIN

#### 4.1 Introduction

In Chapter 3, a cyclic peptide based on the sequence motif of KFAKF (lysine-phenylalanine-alanine-lysine-phenylalanine) was observed to promote *de novo* amyloidosis of human recombinant prion protein (hPrP). It has been hypothesized by other researchers that an unknown protein cofactor, called “protein X”, interacts with the prion protein to cause amyloid misfolding *in vivo*.<sup>28</sup> The identity of protein X has not been established despite decades of research. To explore the relationship between KFAKF-based peptides and physiological cofactors that may interact with the prion protein in a manner consistent with the protein X hypothesis, a set of peptides containing the sequence RFMRF (arginine-phenylalanine-methionine-arginine-phenylalanine) were tested for an ability to induce *in vitro* amyloidosis of hPrP. The RFMRF sequence motif was chosen based on homology to the FMRF sequence of a short neuropeptide that was initially isolated in clams<sup>49</sup>, but later found to have mammalian homologs that are referred to as RF-amide peptides.<sup>35</sup> RF-amide peptides are constitutively expressed in the brains of mammals and play important roles regulating neuroendocrine function.<sup>49</sup> Our

results presented here indicate that peptides containing the sequence RFMRF may indeed facilitate prion amyloidosis.

## **4.2 Results and Discussion**

### *4.2.1 Purification and native folding of recombinant hPrP*

Recombinant human prion protein (hPrP) was expressed in *E. coli* cells and purified from cell lysate using Ni<sup>2+</sup> affinity chromatography, as detailed in Chapter 2. The purity of hPrP obtained in this manner was judged to be greater than 99% by silver staining of samples electrophoresed using SDS-PAGE techniques (see Figure 2.4). The identity of the purified protein was verified as hPrP by western blot analysis using the monoclonal antibody 3F4 (see Figure 2.5). CD spectroscopy demonstrated that the recombinant hPrP was correctly folded into its native state (see Figure 3.1).

### *4.2.2 hPrP amyloidosis induced by peptide homologs to RF-amide neuropeptides*

The ability of small peptides containing the sequence RFMRF to promote amyloidosis of natively folded hPrP was tested by mixing protein and peptide to final concentrations of 4.3  $\mu$ M hPrP and 1 mM peptide in 1X PBS, 0.1% SDS, 0.1% TritonX-100, consistent with the solution conditions used in Chapter 3 for testing peptide-induced hPrP amyloidosis. The peptides tested were synthesized commercially by GenScript (Piscataway, NJ) and are listed in Table 4.1. Each hPrP + peptide sample was incubated at 37°C with periodic and gentle sonication, as described in the Methods (section 2.5.1).

The structural conversion of natively folded recombinant hPrP to amyloid in each sample was tested using multiple amyloid detection techniques. Shown in Figure 4.1 are the results of incubating hPrP with the cyclic peptide cyclo-CGGRFMRFGGC (referred to as peptide-6) for up to 72 hours, as monitored by the fluorescence of Thioflavin T

**Table 4.1.** RF-amide peptide homologs that were synthesized and tested for the ability to promote amyloidosis of recombinant hPrP.

<b>Peptide Name</b>	<b>Peptide Sequence</b>
Peptide-4	RFMRF
Peptide-5	cyclo-CGRFMRFGC
Peptide-6	cyclo-CGGRFMRFGGC

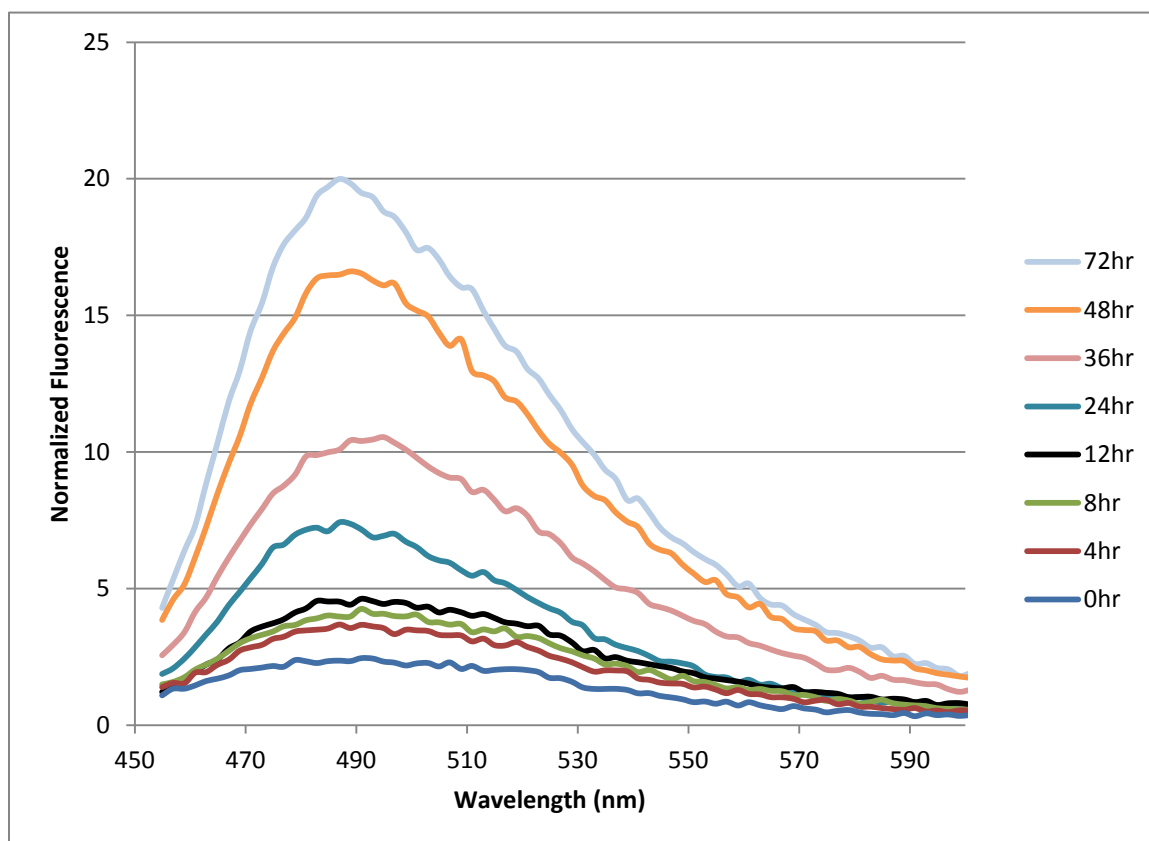


**Figure 4.1. Fluorescence spectra of samples containing hPrP + cyclo-CGGRFMRFGGC, incubated from 0 to 72 hours.** Each sample contained 4.3  $\mu\text{M}$  hPrP, 1 mM cyclo-CGGRFMRFGGC, 1X PBS, 0.1% SDS, 0.1% TritonX-100 and was incubated at 37°C as indicated. 15  $\mu\text{L}$  of each sample was individually mixed with 985  $\mu\text{L}$  of 10  $\mu\text{M}$  ThT, 50 mM glycine, pH 8.5 and its emission spectrum was measured using an excitation wavelength of 442 nm.

(ThT). As can be seen in the figure, at the initial time point (0 hr), there was minimal sample fluorescence suggesting no amyloid was present. Over the course of 72 hours, the sample fluorescence increased substantially, suggesting that amyloid particles formed over time in the sample. Samples containing hPrP only or peptide-6 only showed no fluorescence increase, relative to the initial sample fluorescence, for incubation times up to 48 hours (Figure 4.2). Samples containing hPrP + cyclo-CGRFMRFGC (peptide-5) or hPrP + RFMRF (peptide-4) also gave no detectable fluorimetric signal for amyloid in samples incubated as long as 72 hours (Figure 4.3). These experiments were repeated an additional 2 times, for a total of 3 trials, and displayed good reproducibility. The cumulative results of peptide-6-induced amyloidosis of hPrP as monitored by ThT fluorescence is given in Figure 4.4 for the 3 trials. These data suggest that peptide-6 interacts with recombinant hPrP to promote amyloid misfolding, while the other two synthetic peptides that were tested (peptide-4 and peptide-5) do not.

The peptide-induced misfolding of hPrP into amyloid was also monitored by a Proteinase K (PK) digestion assay. Only samples containing both hPrP and peptide-6, and that were incubated for at least 8 hours, resulted in particles that resisted PK digestion, which are shown in Figure 4.5. The PK-resistant fragment was 16 kDa – consistent with hPrP amyloidosis. Of note, samples incubated for less than 8 hours were fully digested by PK, suggesting that peptide-6 did not inhibit PK activity. Samples containing hPrP + peptide-4 or hPrP + peptide-5 and incubated for up to 72 hours were also fully digested by PK, suggesting no amyloid conversion. Western blot results for samples containing hPrP + peptide-4 and hPrP + peptide-5 incubated for 48 hours are shown in lanes 10 and 11, respectively, of the Figure 4.5 gel image.

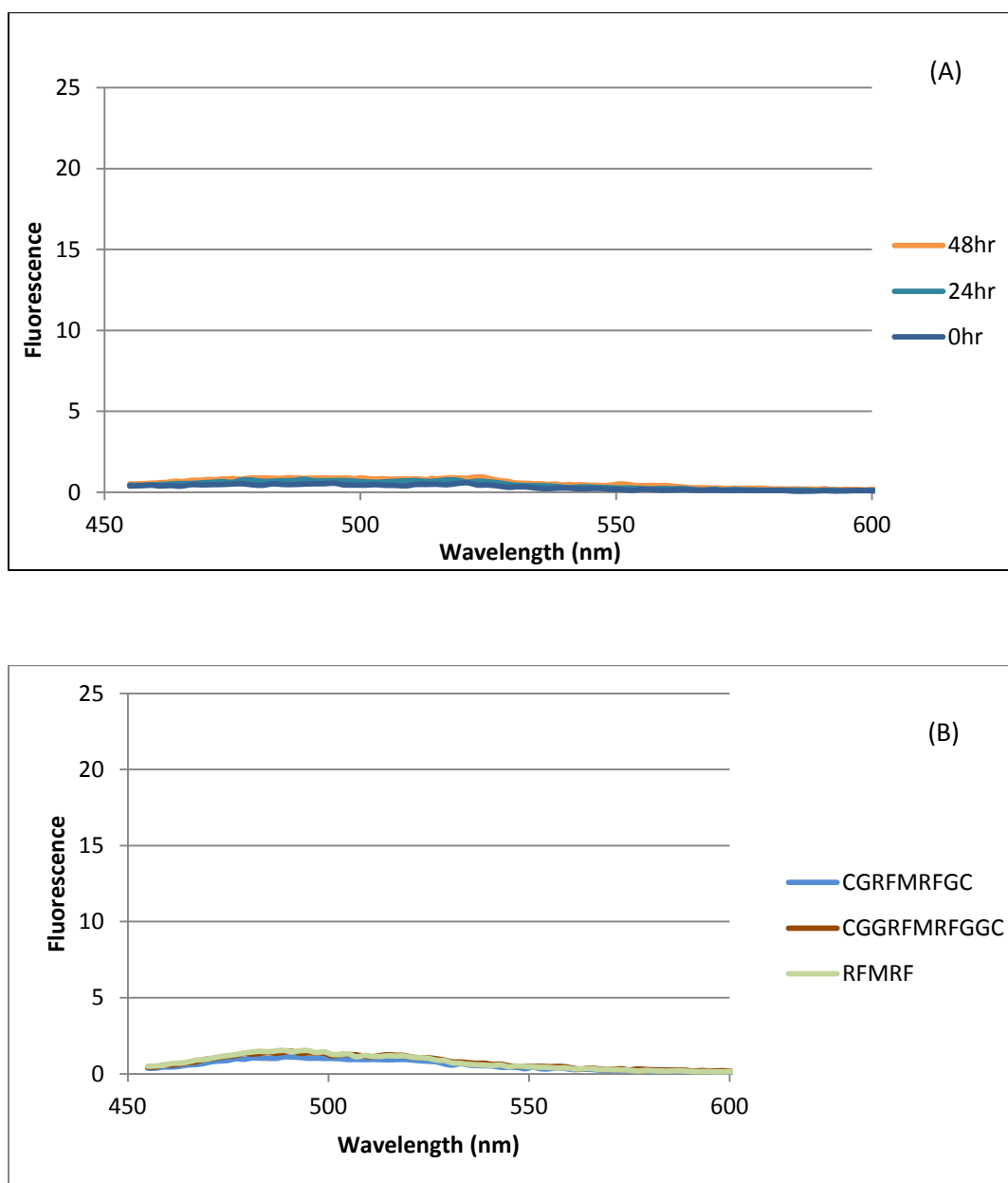


**Figure 4.2. ThT fluorescence when mixed with hPrP only or the synthetic peptides only.** (A) Fluorescence spectra for samples containing 4.3  $\mu\text{M}$  hPrP, 1X PBS, 0.1% SDS, 0.1% TritonX-100 and incubated at 37°C as indicated. 15  $\mu\text{L}$  of each sample was individually mixed with 985  $\mu\text{L}$  of 10  $\mu\text{M}$  ThT, 50 mM glycine, pH 8.5 and its emission spectrum was measured using an excitation wavelength of 442 nm. (B) Fluorescence spectra for samples containing 1X PBS, 0.1% SDS, 0.1% TritonX-100 + 1 mM RMRRF (light green) or + 1 mM cyclo-CGRMRFGC (blue) or + 1 mM cyclo-CGGRMRFGGC (maroon) and incubated at 37°C for 48 hours. 15  $\mu\text{L}$  of each sample was individually mixed with 985  $\mu\text{L}$  of 10  $\mu\text{M}$  ThT, 50 mM glycine, pH 8.5 and its emission spectrum was measured using an excitation wavelength of 442 nm.

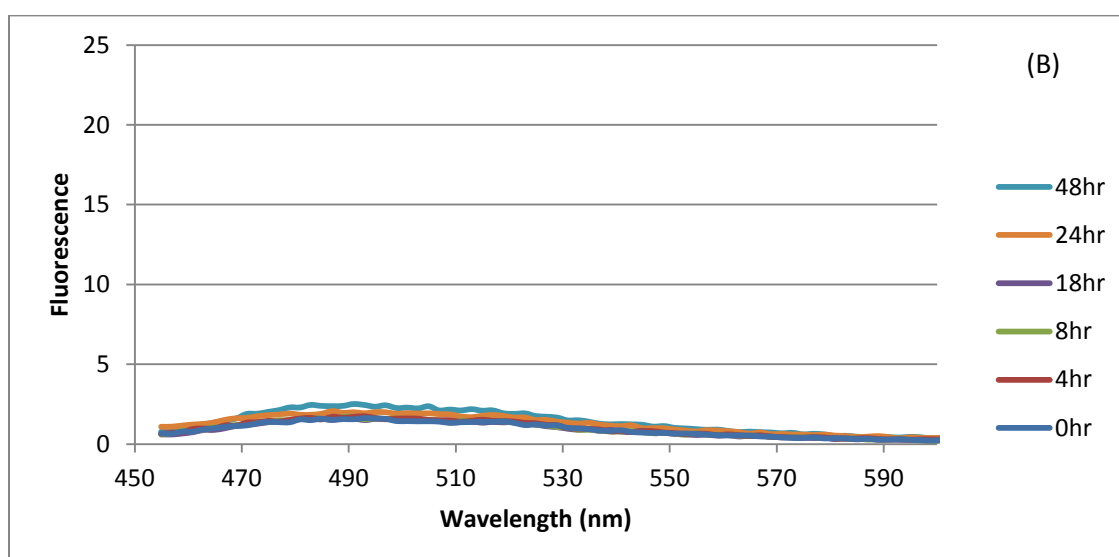
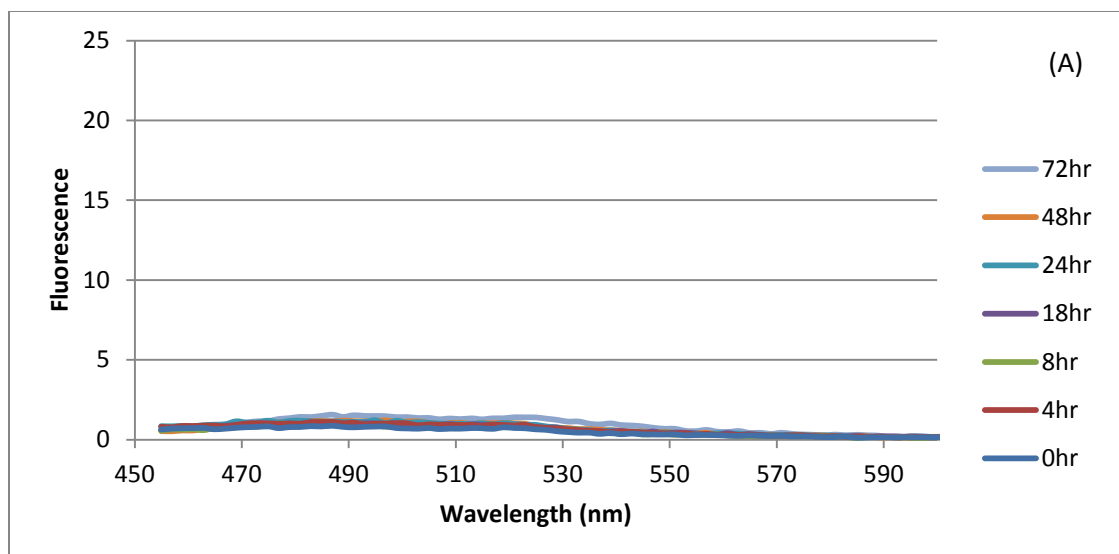


**Figure 4.3. Fluorescence spectra of samples containing hPrP + RFMRF or hPrP + cyclo-CGRFMRFGC, and incubated from 0 to 72 hours.** Each sample contained 4.3  $\mu$ M hPrP, 1X PBS, 0.1% SDS, 0.1% TritonX-100 and was incubated at 37°C as indicated. Samples in (A) included 1 mM RFMRF. Samples in (B) included 1 mM cyclo-CGRFMRFGC. 15  $\mu$ L of each sample was individually mixed with 985  $\mu$ L of 10  $\mu$ M ThT, 50 mM glycine, pH 8.5 and its emission spectrum was measured using an excitation wavelength of 442 nm.

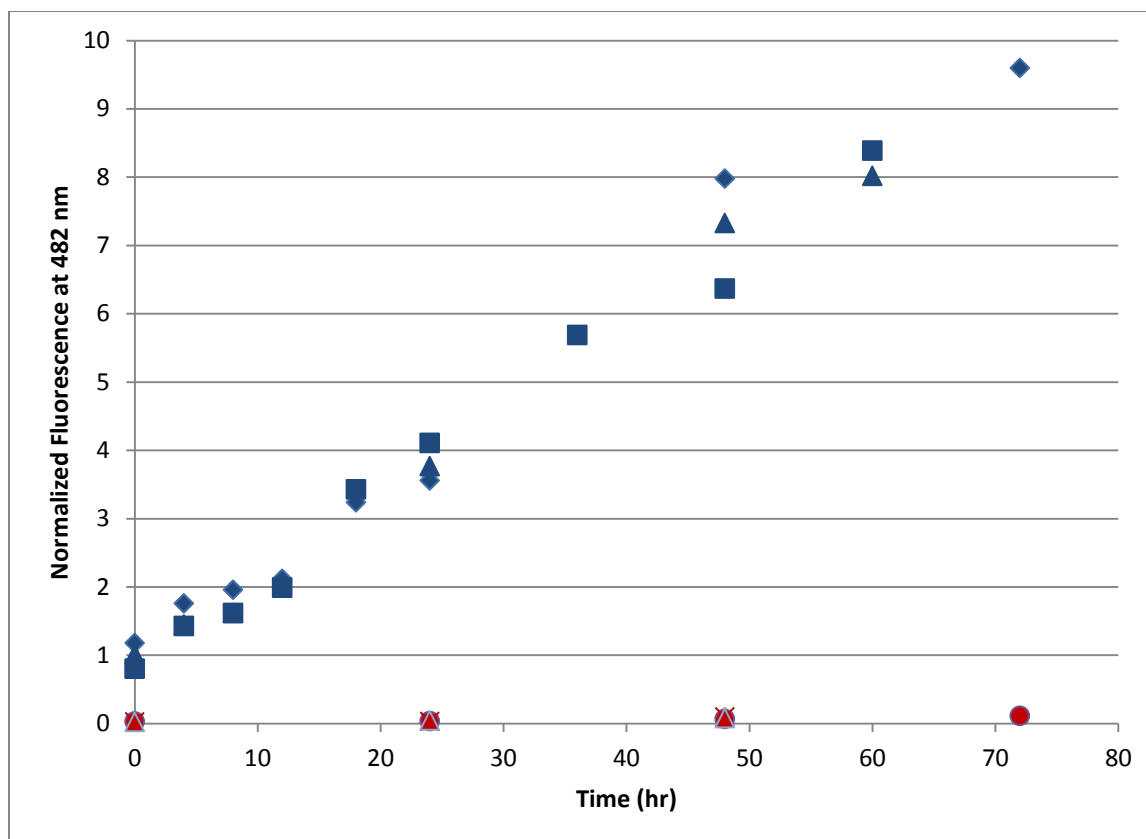


**Figure 4.4. Fluorescence at 482 nm for triplicate samples containing hPrP + cyclo-CGGRFMRFGGC.** Each sample contained 1X PBS, 0.1% SDS, 0.1% TritonX-100 and was incubated at 37°C for the time indicated in the figure. 15  $\mu$ L of each sample was individually mixed with 985  $\mu$ L of 10  $\mu$ M ThT, 50 mM glycine, pH 8.5 and its fluorescence emission at 482 nm was measured using an excitation wavelength of 442 nm. Dark blue symbols represent samples that contained 4.3  $\mu$ M hPrP and 1 mM cyclo-CGGRFMRFGGC; the different symbols (squares, triangles, and diamonds) represent different trial sets. The symbols in red represent control samples that contained 4.3  $\mu$ M hPrP (diamonds, cross marks, and circles) or 1 mM cyclo-CGGRFMRFGGC (triangles, squares, and stars). To compare sample fluorescence measured from different trials performed on different dates, each data point in this figure was normalized to the measured fluorescence at 430 nm for the ThT solution alone (10  $\mu$ M ThT, 50 mM glycine, pH 8.5), due to an excitation wavelength of 342 nm.

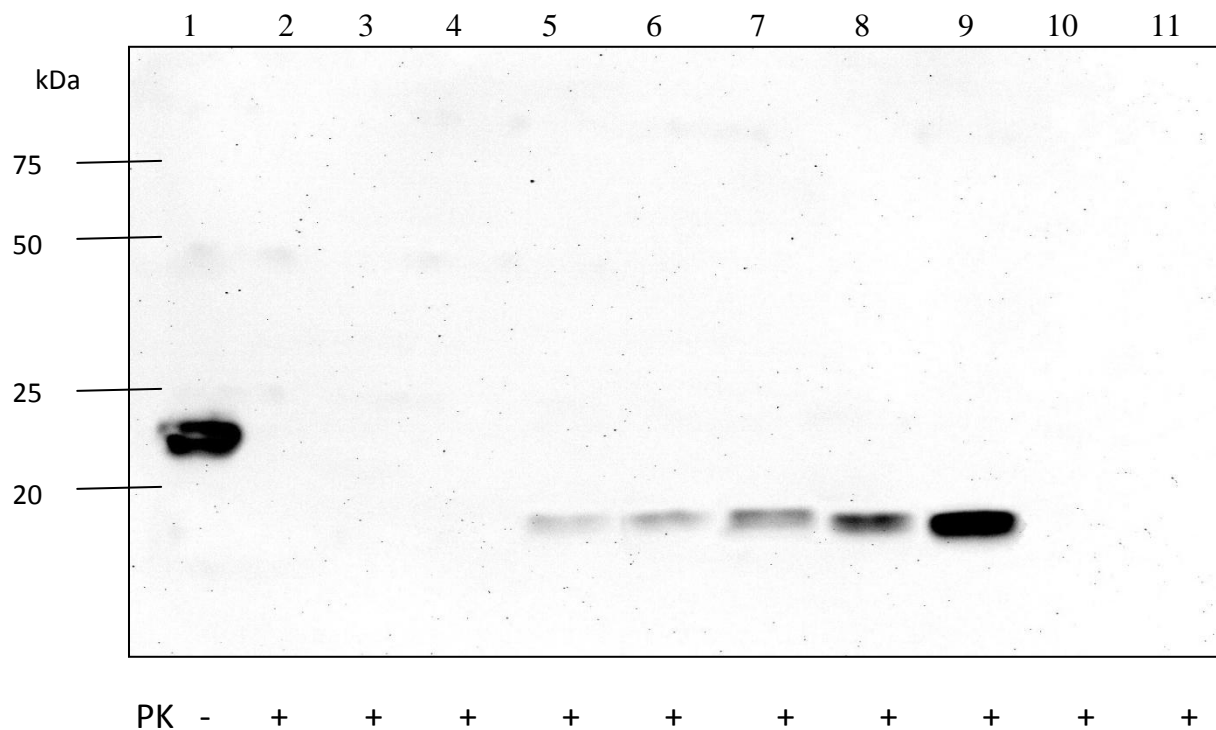


**Figure 4.5. Proteinase K digestion of recombinant hPrP.** Shown is the PK digestion of samples containing 4.3  $\mu$ M hPrP, 1 mM cyclo-CGGRFMRFGGC, 1X PBS, 0.1% SDS, 0.1% TritonX-100 and incubated at 37°C for 0 to 72 hours. Lane 1 is a control, showing an undigested sample without 1 mM cyclo-CGGRFMRFGGC added and at the initial time point (0 hr). Lane 2 is another control, at the 0 hr time point, and without 1 mM cyclo-CGGRFMRFGGC added, but digested by PK. Lanes 3 through 9 show PK digested samples incubated for 0, 4, 8, 18, 24, 48, and 72 hours. Lane 10 shows PK digestion of a sample containing 1 mM RFMRF instead of cyclo-CGGRFMRFGGC and incubated for 48 hours. Lane 11 shows PK digestion of a sample containing 1 mM cyclo-CGRFMRFGC instead of cyclo-CGGRFMRFGGC and incubated for 48 hours. After completion of the western blot protocol, the polyacrylamide gel was stained with coomassie to view molecular weight standards that were electrophoresed in an additional lane. The positions of the molecular weight standards are estimated in the gel image based upon their coomassie-stained positions.

Samples of hPrP + peptide-6 were also tested for amyloid by light scattering (turbidity); the result of which are shown in Figure 4.6. Sample turbidity was observed to increase as the incubation time was increased from 0 to 72 hours, which is consistent with a progressive conversion of natively folded hPrP to amyloid fibrils.

#### 4.2.3 *hPrP amyloidosis through amyloid seeding*

The amyloid particles formed from hPrP:peptide-6 interactions were isolated by centrifugation and then resuspended in 1X PBS for use in trials to test their ability to seed fresh conversion of native hPrP. The results of these seeding experiments are shown in Figure 4.7, where ~ 100 ng of peptide-6-induced hPrP amyloid were mixed with 4.3  $\mu$ M hPrP in 100  $\mu$ L of 1X PBS, 0.1% SDS, 0.1% TritonX-100. The samples were incubated for up to 72 hours and monitored by the same ThT fluorescence assay used in Figure 4.1. The results of these experiments show that at the initial time point (0 hr) the sample contained nearly undetectable amounts of amyloid. After 72 hours of incubation, however, a large increase in sample fluorescence was observed, suggesting extensive conversion of native hPrP to amyloid. Figure 4.8 demonstrates that the turbidity of the sample increased concomitant to the increase in ThT fluorescence, and likewise was consistent with amyloid conversion of native hPrP.

To test if the observed hPrP amyloidosis resulted from dilute amounts of peptide-6 present in the seeded sample, a fresh sample of natively folded hPrP was incubated with 0.1 mM peptide-6 for 72 hours. This is the maximum peptide-6 concentration that could be present in the seeded reactions of Figures 4.7 and 4.8, based on the protocol used (see Chapter 2, section 2.5.2). Figure 4.9 demonstrates that no significant amyloid conversion was observed in samples of hPrP + 0.1 mM peptide-6, even after the sample was

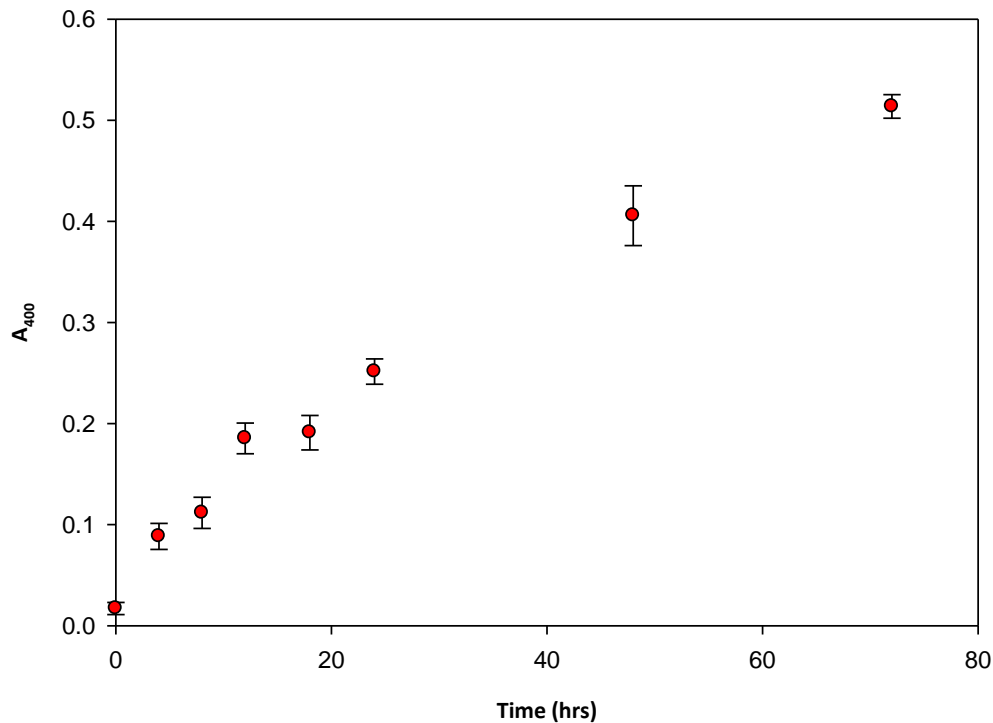


**Figure 4.6. Turbidity of samples containing hPrP + cyclo-CGGRFMRFGGC, incubated from 0 to 72 hours.** Each sample contained 4.3  $\mu$ M hPrP, 1 mM cyclo-CGGRFMRFGGC, 1X PBS, 0.1% SDS, 0.1% TritonX-100 and was incubated at 37°C as indicated. The absorbance of each sample was measured at 400 nm ( $A_{400}$ ). Each data point in the figure is an average from the experiment being performed in triplicate. The error bars represent the standard deviation in each averaged value.

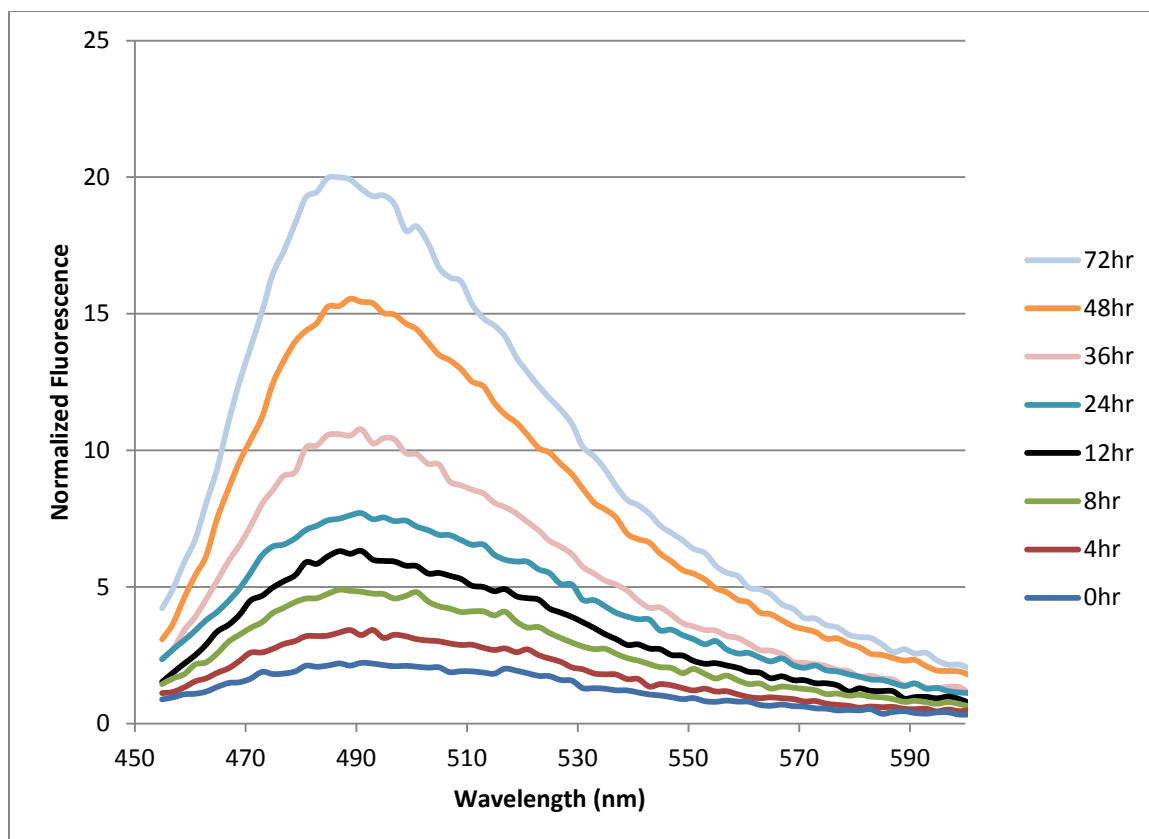


**Figure 4.7. Fluorescence spectra of samples containing hPrP + ~ 100 ng hPrP amyloid, incubated from 0 to 72 hours.** Each sample consisted of 100  $\mu\text{L}$  of 4.3  $\mu\text{M}$  hPrP, 1X PBS, 0.1% SDS, 0.1% TritonX-100 mixed with ~ 100 ng peptide-6-induced hPrP amyloid and was incubated at 37°C as indicated. 15  $\mu\text{L}$  of each sample was individually mixed with 985  $\mu\text{L}$  of 10  $\mu\text{M}$  ThT, 50 mM glycine, pH 8.5 and its emission spectrum was measured using an excitation wavelength of 442 nm.

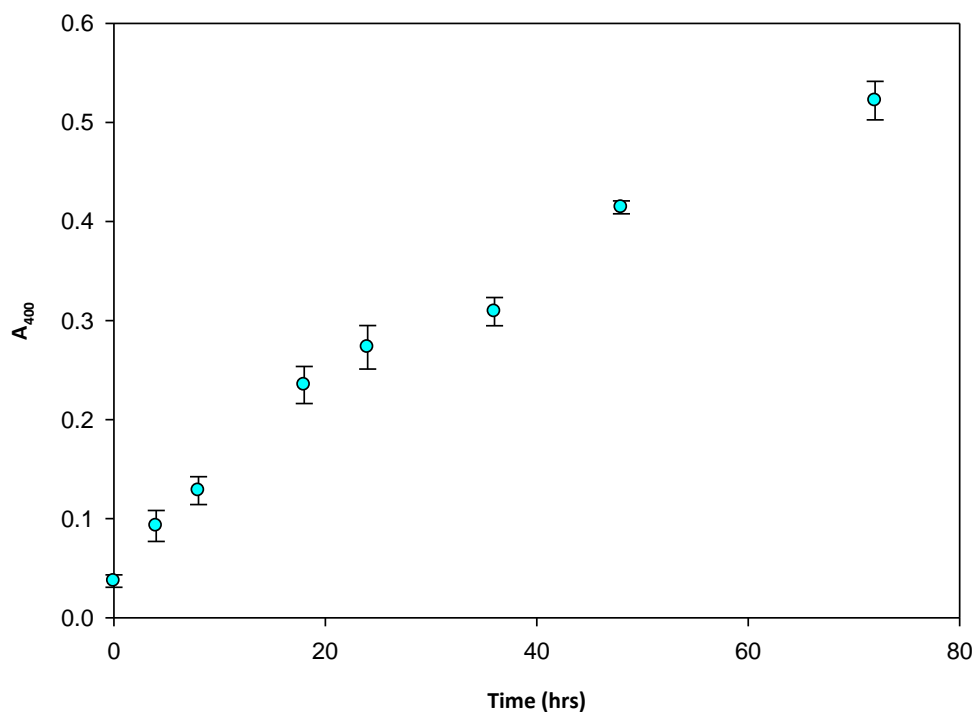


**Figure 4.8. Turbidity of samples containing hPrP + ~ 100 ng hPrP amyloid, incubated from 0 to 72 hours.** Each sample consisted of 100  $\mu\text{L}$  of 4.3  $\mu\text{M}$  hPrP, 1X PBS, 0.1% SDS, 0.1% TritonX-100 mixed with ~ 100 ng peptide-6-induced hPrP amyloid and was incubated at 37°C as indicated. The absorbance of each sample was measured at 400 nm ( $A_{400}$ ). Each data point in the figure is an average from the experiment being performed in triplicate. The error bars represent the standard deviation in each averaged value.

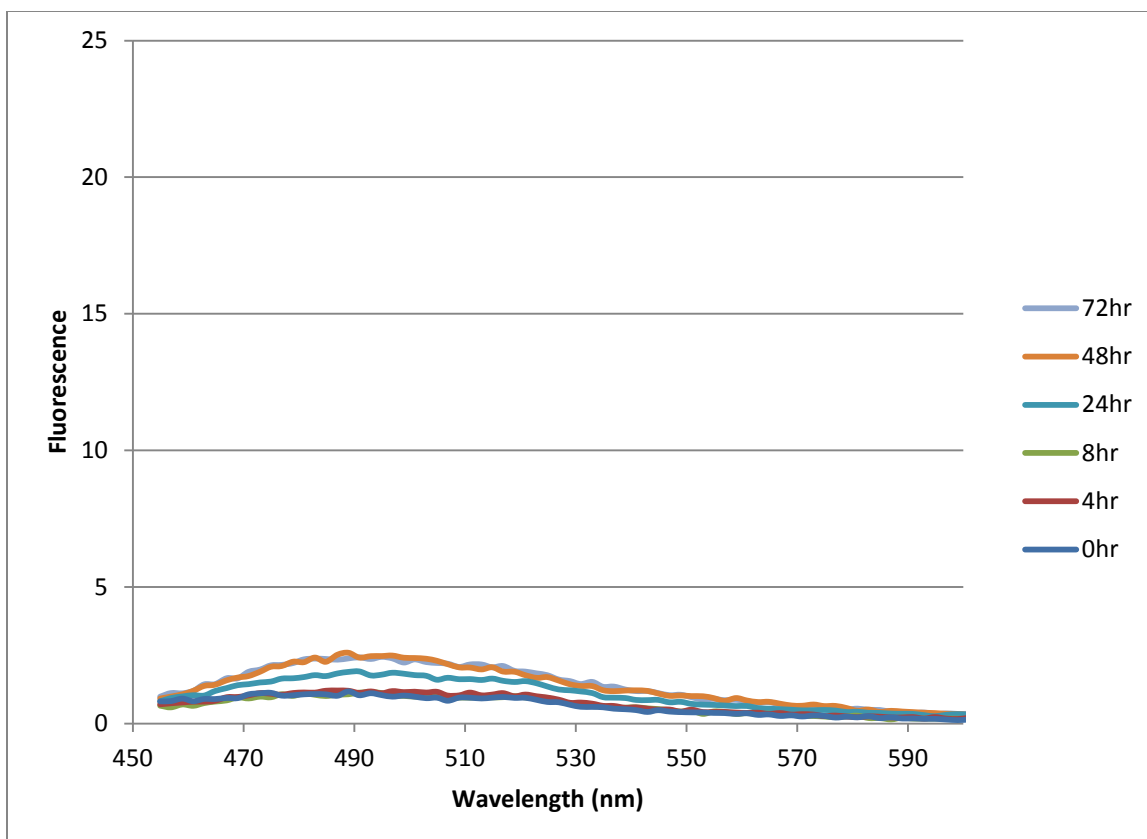


**Figure 4.9. Fluorescence spectra of samples containing hPrP + 0.1 mM cyclo-CGGRFMRFGGC, incubated from 0 to 72 hours.** Each sample contained 4.3  $\mu\text{M}$  hPrP, 0.1 mM cyclo-CGGRFMRFGGC, 1X PBS, 0.1% SDS, 0.1% TritonX-100 and was incubated at 37°C as indicated. 15  $\mu\text{L}$  of each sample was individually mixed with 985  $\mu\text{L}$  of 10  $\mu\text{M}$  ThT, 50 mM glycine, pH 8.5 and its emission spectrum was measured using an excitation wavelength of 442 nm.

incubated for 72 hours. These results suggest that hPrP amyloidosis induced by the amyloid seeds were not the result of dilute amounts of peptide-6 present in the sample.

### 4.3 *Conclusions*

In chapter 3, it was shown that a small cyclic peptide containing the sequence KFAKF could promote the self-assembly of recombinant hPrP into amyloid fibrils. Based on that success, synthetic peptides containing the sequence RFMRF were also tested for amyloidosis-inducing capabilities when incubated with recombinant hPrP. The RFMRF-containing synthetic peptides were tested for two main reasons: 1) they provided a simple variation from the original sequence motif and a logical first step toward exploring more expansive sequence variations, and 2) the sequence homology to RF-amide peptides provided an initial test toward investigating potential physiological cofactors of the prion diseases. Other researchers have hypothesized physiological cofactors to the prion disorders<sup>28</sup>, but none have been found to date. Whether or not RF-amide peptides contribute *in vivo* to the prion disorders is currently unknown. Our results presented here provide evidence that RF-amide peptides are potential prion disease cofactors. It is important to note that regardless of any potential linkage between RF-amide peptides and prion diseases, a recombinant hPrP-peptide system has been developed to explore such issues as well as to investigate the molecular interactions that facilitate prion amyloidosis, which was the primary goal of this thesis.

## REFERENCES

1. Scott, H. *Internet J. Neurol.* [Online] **2009**, 11 (2), 1-16.
2. Soto, C. *Neuroscience* **2003**, 4, 49-60.
3. Gruschus, J.M. *Amyloid* **2008**, 15 (3), 160-165.
4. Soto, C. *Lancet Neurol.* **2007**, 6 (4), 294-295.
5. Sideras, K.; Gertz, M.A. *Adv. Clin. Chem.* **2009**, 47, 1-44.
6. Kushnirov, V.V.; Alexandrov, I.M.; Mitkevich, O.V.; Shkundina, I.S.; Ter-Avanesyn, M.D. *Methods* **2006**, 39, 50-55.
7. Soto, C.; Kascsak, R.J.; Saborío, G.P.; Aucouturier, P.; Wisniewski, T.; Prelli, F.; Kascsak, R.; Mendez, E.; Harris, D.A.; Ironside, J.; Tagliavini, F.; Carp, R.I.; Frangione, B. *Lancet* **2000**, 355 (9199), 192-197.
8. Saá, P.; Castilla, J.; Soto, C. *Science* **2006**, 313, 92-94.
9. Mok, K.H.; Pettersson, J.; Orrenius, S.; Svanborg, C. *Biochem. Biophys. Res. Commun.* **2007**, 354 (1), 1-7.

10. Pruisner, S.B.; Scott, M.R.; DeArmond, S.J.; Cohen, F.E. *Cell* **1998**, 93, 337-348.
11. Glabe, C.G. *J. Biol. Chem.* **2008**, 283, 29639-29643.
12. Zhou, Z.; Fan, J.; Zhu, H.; Shewmaker, F.; Yan, X.; Chen, X.; Chen, J.; Xiao, G.; Guo, L.; Liang, Y. *J. Biol. Chem.* **2009**, 284 (44), 30148-58.
13. Soto, C.; Satani, N. *Trends Mol. Med.* **2011**, 17 (1), 14-24.
14. Cisse, M.; Mucke, L. *Nature* **2009**, 457, 1090-1091.
15. Kaye, R.; Head, E.; Thompson, J.L.; McIntire, T.M.; Milton, S.C.; Cotman, C.W.; Glabe, C.G. *Science* **2003**, 300, 486-489.
16. Xiaojun, L. Structure of Prion Protein Amyloid Fibrils as Determined by Hydrogen/Deuterium Exchange. Ph.D. Dissertation, Case Western Reserve University, Cleveland, OH, 2008.
17. Pruisner, S.B. *Proc. Natl. Acad. Sci.* **1998**, 95, 13363-13383.
18. Sheehan, D. *Physical Biochemistry: Principles and Applications*, 2; Wiley-Blackwell: Chippenham, Wiltshire, 2009; pp 221-226.
19. Nandi, P.K.; Nicole, J.C. *J. Mol. Biol.* **2004**, 334, 827-837.
20. Dobson, C.M. *Trends Biochem. Sci.* **1999**, 9, 329-332.

21. Ghahghaei, A.; Faridi, N. *J. Biomed. Sci. Eng.* **2009**, 2, 345-358.
22. Baskakov, I.V.; Lagname, G.; Gryczynski, Z.; Pruisner, S.B. *Protein Sci.* **2004**, 13, 586-595.
23. Soto, C.; Castilla, J. *Nat. Med.* **2004**, 10, S63-S67.
24. Soto, C.; Estrada, L.; Castilla, J. *Trends Biochem. Sci.* **2006**, 31 (3), 150-155.
25. Voet, D.; Voet, J.G.; Pratt, C.W. *Fundamentals of Biochemistry: Life at the Molecular Level*, 3, John Wiley and Sons, Inc.: Hoboken, NJ, 2008; pp 624-629.
26. Zhang, J. *J. Theor. Biol.* **2011**, 269, 88-95.
27. Liu, T.; Whitten, S.T.; Hilser, V.J. *Proc. Natl. Acad. Sci. USA* **2007**, 104, 4347-4352.
28. Soto, C. *Trends Biochem. Sci.* **2011**, 36 (3), 151-158.
29. Zahn, R.; Liu, A.; Lühns, T.; Riek, R.; Schroetter, C.V.; García, F.L.; Billeter, M.; Calzolari, L.; Wider, G.; Wüthrich, K. *P. Natl. Acad. Sci.* **2000**, 97 (1), 415-150.
30. Saborio, G.P.; Permanne, B.; Soto, C. *Nature* **2001**, 411, 810-813.
31. Kupfer, L.; Hinrichs, W.; Groschup, M.H. *Curr. Mol. Med.* **2009**, 9, 826-835.
32. Castilla, J.; Saá, P.; Hetz, C.; Soto, C. *Cell* **2005**, 121, 195-206.

33. Castilla, J.; Gonzalez-Romero, D.; Saá, P.; Morales, R.; De Castro, J.; Soto, C. *Cell* **2008**, 134, 757-768.
34. Masel, J.; Jansen, V.A. *Biophys. Chem.* **2000**, 88, 47-59.
35. Bechtold, D.A.; Luckman, S.M. *J. Endocrinol.* **2007**, 192, 3-15.
36. Altschul, S.F.; Gish, W.; Miller, W.; Myers, E.W.; Lipman, D.J. *J. Mol. Biol.* **1990**, 215, 403-410.
37. Schwarze-Eicker, K.; Kayvani, K.; Görtz, N.; Westaway, D.; Sachser, N.; Paulus, W. *Neurobiol. Aging* **2005**, 26, 1177-1182.
38. Welch, M.; Govindarajan, S.; Ness, J.E.; Villalobos, A.; Gurney, A.; Minshull, J.; Gustafsson, C. *PLoS One* **2009**, 4 (9), e7002.
39. Gentz, R.; Bujard, H. *J. Bacteriol* **1985**, 164 (1), 70-77.
40. Nicolas, O.; Gavín, R.; del Río, J.A. *Brain Res. Rev.* **2009**, 61, 170-184.
41. Switzer, R.C.; Merrill, C.R.; Shifrin, S. *Anal. Biochem.* **1979**, 98, 231-237.
42. Gill, S.C.; von Hippel, P.H. *Anal. Biochem.* **1989**, 182, 319-326.
43. Caughey, B.; Horiuchi, M.; Demaimay, R.; Raymond, G.J. *Methods Enzymol.* **1999**, 309, 122-133.

44. Gasset, M.; Baldwin, M.A.; Lloyd, D.H.; Gabriel, J.M.; Holtzman, D.M.; Cohen, F.; Fletterick, R.; Pruisner, S.B. *Proc. Natl. Acad. USA* **1992**, 89, 10940-10944.
45. LeVine, H. III *Methods in Enzymol.* **1999**, 309, 274-284.
46. De Simone, A.; Zagari, A.; Derreumaux, P. *Biophys. J.* **2007**, 93, 1284-1292.
47. Pan, K.; Baldwin, M.; Nguyen, J.; Gasset, M.; Serban, A.; Groth, D.; Mehlhorn, I.; Huang, Z.; Fletterick, R.J.; Cohen, F.E.; Pruisner, S.B. *Proc. Natl. Acad. Sci. USA* **1993**, 90, 10962-10966.
48. Come, J.H.; Fraser, P.E.; Lansbury, P.T. *Proc. Natl. Acad. Sci. USA* **1993**, 90, 5959-5963.
49. Kriegsfeld, L.J.; *Horm. Behav.* **2006**, 50, 655-666.

## VITA

Melody Christine Adam was born on March 15, 1984, the daughter of William Stewart Adam and Kathleen Augustus Reeves Adam. After completing her work at Stratford High School, Houston, Texas, in 2002, she entered Stephen F. Austin State University. Her first year there she excelled in her studies, and became acknowledged on the Presidential Honor Roll. The following two years she consecutively received the Outstanding Achievement Award, provided by the Chemistry Department. While working on her undergraduate degree, Melody was accepted into the following honors programs: School of Honors, National Society of Collegiate Scholars, National Dean's List, and Gamma Sigma Epsilon Chemistry Honor Society. She was also a member of the Chemistry Club and the American Marketing Association. Lastly, she worked as a Supplemental Instruction Leader by tutoring general chemistry students for three semesters. Melody received the degree of Bachelor of Science in Chemistry from SFA in May 2008. Upon graduation, she moved to California, where she became employed as a wine chemist intern at J. Lohr Winery. During this time, she was promoted to Malolactic Tracker by the head winemaker. In June, 2009, Melody moved back to Texas, where she entered the Graduate College of Texas State University-San Marcos. While working on her graduate degree, she worked as a Teacher's Assistant for Organic II and Quantitative Analysis laboratories.

Permanent Address: 6715 Hertford Park Dr.

Houston, TX 77084

This thesis was typed by Melody C. Adam.